PROBABILITY OF SUFFICIENCY OF SOLVENCY II RESERVE RISK MARGINS: PRACTICAL APPROXIMATIONS

BY

ERIC DAL MORO AND YURIY KRVAVYCH

ABSTRACT

The new Solvency II Directive and the upcoming IFRS 17 regime bring significant changes to current reporting of insurance entities, and particularly in relation to valuation of insurance liabilities. Insurers will be required to valuate their insurance liabilities on a risk-adjusted basis to allow for uncertainty inherent in cash flows that arise from the liability of insurance contracts. Whilst most European-based insurers are expected to adopt the Cost of Capital approach to calculate reserve risk margin — the risk adjustment method commonly agreed under Solvency II and IFRS 17, there is one additional requirement of IFRS 17 to also disclose confidence level of the risk margin.

Given there is no specific guidance on the calculation of confidence level, the purpose of this paper is to explore and examine practical ways of estimating the risk margin confidence level measured by Probability of Sufficiency (PoS). The paper provides some practical approximation formulae that would allow one to quickly estimate the implied PoS of Solvency II risk margin for a given non-life insurance liability, the risk profile of which is specified by the type and characteristics of the liability (e.g. type/nature of business, liability duration and convexity, etc.), which, in turn, are associated with

- the level of variability measured by Coefficient of Variation (CoV);
- the degree of Skewness per unit of CoV; and
- the degree of Kurtosis per unit of CoV^2.

The approximation formulae of PoS are derived for both the standalone class risk margin and the diversified risk margin at the portfolio level.

KEYWORDS

IFRS 17, IFRS confidence level of Solvency II risk margins, cost of capital approach, probability of sufficiency, approximations.

Astin Bulletin 47(3), 737-785. doi: 10.1017/asb.2017.12

1. Introduction

In the integrated actuarial and financial valuation, liabilities are generally evaluated using the market-consistent valuation, which ultimately is equivalent to taking the *Best Estimate*[1] and adding a *Risk Margin* on top of it either implicitly or explicitly (see Babbel *et al.*, 2002; Bühlmann, 2004; Møller and Steffensen, 2007; Wüthrich *et al.*, 2007). In an ideal situation when the market is complete, the liabilities are fully hedgeable and their market-consistent value can be inferred directly from capital markets using a replicating portfolio approach, or equivalently, a mark-to-market approach. In such a case of perfect hedge, the market-consistent value is nothing but a risk-adjusted expected value of future liability cashflows taken under a unique equivalent martingale measure. Such a risk-adjusted mean value of future liability cashflows would then implicitly allow for a risk margin. However, in reality, insurance risks are non-hedgeable in their nature and perfect replication is impossible as there is no established deep liquid market for trading insurance liabilities, or equivalently, insurance markets are incomplete. In this situation, there is no unique equivalent martingale measure and the valuation suffers from an overabundance of alternatives. One of the natural ways of arriving at the market-consistent value of liabilities in incomplete markets is to use various optimal hedging techniques that minimise the variance of the payoff risk. Examples of optimal hedging include mean-variance hedging, quantile hedging, indifference pricing (see Møller and Steffensen, 2007) and minimum-entropy martingale transform (see Møller, 2004).

Another alternative way of arriving at the market-consistent value of non-headgeable liabilities in insurance markets is to use a mark-to-model approach under which the liabilities could be transferred to a willing rational counterparty at a price that would fully reflect the market/buyer's perception of risk. The price for assuming risk from insurance liability portfolio transfer comes in the form of an economic risk margin that is explicitly calculated and stacked on top of the best estimate. In this case, the risk margin is equivalent to the "current exit value" defined by the IASB (see IASB, 2007) as *"The amount the insurer would expect to pay at the reporting date to transfer its remaining contractual rights and obligations immediately to another entity"*.

Under both the new Solvency II Directive and the upcoming IFRS 17 regime,[2] insurers will be required to evaluate their insurance liabilities on a market-consistent basis allowing for uncertainty inherent in cash flows that arise from the liability of insurance contracts. In particular, Solvency II mandates the so-called Cost of Capital (CoC) approach under which the market-consistent risk margin is calculated as the hypothetical cost of regulatory capital necessary to runoff or transfer all liabilities following the financial distress of the insurer. Whilst in principle the use of any market-consistent valuation approach is allowed under the IFRS 17, in view of Solvency II it is expected that most European-based insurers will adopt the CoC approach to calculating reserve risk margin. However, the IFRS 17 introduces additional complexity to the market-consistent valuation requirements compared to Solvency II

— it also requires to disclose the confidence level to which the risk margin corresponds.

The notion of the confidence level of risk margin is not new and has been in use in actuarial practice in various forms, mainly for setting risk margin with reference to the level of prudence in liability valuation. It also resonates with some traditional approaches to allowing for reserve uncertainty/variability in liability valuation. For example, in Australia, the non-life technical provisions are required by APRA[3] (see APRA Prudential Standards GPS 310, 2010) to be set with the minimum of 75% of Probability of Sufficiency (PoS),[4] in which case the implied risk margin is the difference between the 75th percentile of liability distribution profile and the central estimate.[5] In general, the PoS itself is a measure of prudence in liability valuation:

- PoS below 50% indicates the technical provisions are set below the central estimate (under-reserved position);
- PoS of 50% to 60% indicates the technical provisions are set approximately at the level of central estimate (weak prudence);
- PoS of around 75% indicates that technical provisions are set so that likely (i.e. up to 1-in-4 years) reserve deteriorations above the central estimate are fully absorbed by the technical provisions (adequate prudence); and
- PoS above 75% indicates that the technical provisions could also absorb some of unlikely reserve deteriorations above the central estimate (strong prudence).

Given that there is no specific guidance on the calculation of confidence level, the purpose of this paper is to examine the risk margin confidence (prudence) measured by PoS. The paper provides some practical approximation formulae that would allow one to quickly estimate the implied PoS of Solvency II risk margin for a given non-life insurance liability, the risk profile of which is specified by the type and characteristics of the liability (e.g. type/nature of business, liability duration and convexity, etc.), which, in turn, are associated with the following:

- the level of variability measured by Coefficient of Variation (CoV);
- the degree of Skewness per unit of CoV, i.e. Skewness-to-CoV (SC) ratio; and
- the degree of Kurtosis per unit of CoV^2, i.e. Kurtosis-to-CoV^2 (KCsq) ratio.

The approximation formulae of PoS are derived for both the standalone class risk margin and the diversified risk margin at the portfolio level.

The structure of this paper is as follows. In Section 2, we define and outline the notions of reserve risk, its profile and risk margin, and provide the key assumptions made in this research.

In Section 3, we focus on providing practical approximation formulae for PoS of Solvency II risk margin of a standalone reserving class. Here, the PoS, being an inverse-quantile measure of the risk profile of the single reserving class, is approximated using the two specific approximations: (1) the *Cornish–Fisher (C-F)* approximation (see Fisher and Cornish, 1960); and (2) the *Bohman-Esscher*

(B-E) approximation (see Bohman and Esscher 1963, 1964). The C-F approximation is the quantile approximation of the non-normal distribution by a polynomial of a standard normal quantiles utilising the distribution's moments. The C-F type of approximation formulae for PoS are derived separately for two different cases: (1) when utilising only CoV and skewness of the non-normal distribution; and (2) when utilising its CoV, skewness and kurtosis. The B-E approximation is the inverse-quantile (distribution) approximation of the non-normal distribution by a transformed Gamma distribution utilising the CoV and skewness of the non-normal distribution. The obtained PoS approximations are compared by analysing their quality. The results of the approximation quality analysis revealed that in most practical situations the approximations utilising CoV and skewness only, like B-E and C-F Quadratic approximations, are of fairly good quality, and that only in very rare extreme situations, when the reserve risk profile is overly skewed and leptokurtotic, the kurtosis also becomes a significant driver of the quality of approximation.

In Section 4, we provide approximations of PoS of Solvency II risk margin of a portfolio consisting of multiple reserving classes. In general, the derivation of the distribution of aggregate risk at the portfolio level is to a large extent associated with dependence modelling uncertainty (see, e.g., Embrechts and Jacobsons, 2016). In this paper, we consider a Gaussian dependence structure for aggregating risks[6] and estimate the first four moments of the aggregate reserve risk profile using the *Fleishman* approximation[7] (see Fleishman, 1978). The derived moments are further used to approximate the PoS of the diversified risk margin at the portfolio level by utilising formulae obtained in Section 3.

In Section 5, we discuss practical implementations of the PoS approximations and provide numerical examples. Finally, brief conclusions are given in Section 6.

2. Reserve risk profile and risk margin - background and general assumptions

2.1. Reserve risk profile characteristics

Reserve risk and its carrier. Under Solvency II, the *"risk"* is generally defined as a possibility of having adverse performance result (insurance, investment, or company's overall result) that results in "low capital performance" (i.e. a return on capital below the shareholders opportunity CoC) and/or erosion of current shareholders value (i.e. capital consumptions).[8] In particular, the reserve risk is the risk that provisions for past exposures will be inadequate to meet the ultimate costs when the business is run off to extinction. The risk of reserves developing other than expected (booked provisions) is significant for non-life insurers, especially for long tail lines of business. Here, the reserve provisions are generally booked at the *Best Estimate (BE)* plus *Risk Margin*, where the risk margin plays the role of safety load reflecting the uncertainty in reserve

https://doi.org/10.1017/asb.2017.12 Published online by Cambridge University Press

best estimate. The role of the risk margin is further explained in greater detail in Section 2.2.

The risk is often distinguished from its carrier, which is defined as a random variable. In the case of reserve risk, its carrier is naturally defined as the *reserve value*, which is random due to random nature of claims frequency and severity and also random time lags between (a) the date the insurance event occurs and the date it is reported; and (b) the date it is reported and the date it is eventually settled. Because these time lags, along with underlying claim frequencies and severities, are stochastic, booked claims liabilities have substantial risk that their actual value realised in the future will adversely deviate from the expected value (booked provisions).

Assumption 1. It is the distribution of the reserve risk carrier that characterises the reserve risk, and in this paper it is referred to as the *"reserve risk profile"*.

Reserve risk profile: differentiation by type of business class. In practice, non-life reserving actuaries often use CoV as the measure of riskiness of modelled reserves. For example, personal lines like motor and home are short tail business lines and exhibit relatively lower CoV when compared to long tail classes like commercial liability. However, CoV alone cannot explain all the characteristics of the reserve risk profile, and thus higher moments of reserve distribution like skewness and kurtosis would be required to properly capture (a) the degree of asymmetry of odds towards adverse reserve realisations, and (b) heavy-tailedness of the reserve distribution.

In general, the parametric distributions commonly used in insurance for reserving and loss modelling are of a special type:

- they are often defined by two parameters — the *scale parameter* and the *shape parameter*; and
- their shape is totally driven by a single parameter — their shape parameter.

Equivalently, those two-parameter distributions are such, that when scaled by their mean (location), would have a unique fixed location (unit mean) and variable shape dependent on the shape parameter only, i.e. the distribution of the following random variable Y is a single-parameter distribution and its shape is defined by the shape parameter of X:

$$Y = \frac{1}{m_X} X = 1 + \mathrm{CoV}_X \cdot \widetilde{X}, \tag{1}$$

where $\widetilde{X} = \frac{X - m_X}{m_X \mathrm{CoV}_x}$ and m_X and CoV_X are the mean and CoV of X, respectively.

In this paper, we focus only on the class of two-parameter distributions with *single shape parameter* and denote it by $\mathcal{SSP}$. Examples of two-parameter distributions of $\mathcal{SSP}$ type include[9] Gamma, Inverse-Gaussian (Wild), Log-Normal, Dagum, Suzuki, Exponentiated-Exponential (Verhulst), Inverse-Gamma (Vinci), Birnbaum–Saunders, Exponentiated-Fréchet and

Log-Logistic. It should be noted that not all two-parameter distributions are of $\mathcal{SSP}$ type, and an immediate example of that would be the Log-Gamma distribution defined on the positive real line each of the two parameters of which would drive both the location/scale and the shape of the distribution at the same time.

As illustrated above in (1), for any distribution of $\mathcal{SSP}$ type its shape in general and its CoV in particular are defined by the distribution's shape parameter only. Also, it is a known fact from the Distribution Analysis of the Probability Theory that any analytical cumulative distribution function can be expanded using the C-F expansion (cf. Fisher and Cornish, 1960), which utilises the distribution's skewness, kurtosis[10] and other relative moments of higher order to fully explain its shape. In the case of random variable $\widetilde{X}$, the shape of its distribution is completely explained by the skewness, kurtosis and other relative moments of higher order of X. This implies that all relative moments of third order and higher of any distribution of $\mathcal{SSP}$ type are completely defined by its shape parameter.

Therefore, the distinctive features of the distributions of $\mathcal{SSP}$ type are as follows:

- their shape parameter is a function of CoV;
- their any higher order statistic is fully determined by the shape parameter and hence is a function of CoV, and in particular
  - relative skewness measured by SC ratio is a function of CoV;
  - relative kurtosis measured by KCsq ratio is a function of CoV^2;
- if the $\mathcal{SSP}$ distribution belongs to a certain parametric family (e.g. Log-Normal, Gamma or any other parametric family from $\mathcal{SSP}$), then scaling it by its mean preserves the parametric family it belongs to and its shape parameter, i.e. if $X \sim F_{u,v}$ with mean m_X and standard deviation s_X, scale parameter u and shape parameter v, then $Y = \frac{1}{m_X} X \sim F_{u',v}$ with mean 1 and standard deviation CoV_X.

The latter feature also implies that

$$F_{u,v}(x) = F_{u',v}\left(\frac{x}{m_X}\right). \tag{2}$$

The $\mathcal{SSP}$ distributions can be split into three main categories:

- *Moderately skewed distributions* ($1.5 < \text{SC} \leqslant 3$)
  - Gamma;
  - Suzuki — the distribution admits only CoV $\gtrapprox$ 53%;
  - Inverse-Gaussian[11] (Wald);
  - Exponentiated-Exponential (Verhulst) for CoV $> 40\%$;
- *Significantly skewed distributions* ($3 < \text{SC} \leqslant 4$)
  - Log-Normal for CoV $\leqslant 100\%$;
  - Exponentiated-Exponential (Verhulst) for CoV $\in (30\%, 40\%)$;

https://doi.org/10.1017/asb.2017.12 Published online by Cambridge University Press

- *Extremely skewed distributions* (SC > 4)
  - Inverse-Gamma (Vinci), includes Inverse-Chi-Squared;
  - Birnbaum–Saunders;
  - Log-Logistic (Fisk);
  - Exponentiated-Exponential (Verhulst) for CoV < 30%;
  - Exponentiated-Fréchet.

The parametric distribution commonly used in reserving is the Log-Normal distribution (e.g., see Bateup and Reed, 2001; FINMA, 2006; Taylor, 2006; CEIOPS, 2010). Its skewness and kurtosis are respectively defined by corresponding ratios:

$$\mathrm{SC} = 3 + \mathrm{CoV}^2 > 3, \tag{3}$$

$$\mathrm{KCsq} = 16 + 15\mathrm{CoV}^2 + 6\mathrm{CoV}^4 + \mathrm{CoV}^6 > 16. \tag{4}$$

However, the Log-Normal distribution, whilst being suitable for modelling a wide range of skewed medium- to heavy-tailed risk profiles, is still not the best one for modelling risk profiles with low skewness and light tail or excessively high skewness and heavy tail.

Assumption 2. This paper considers the following four distributional *Domains of Attraction (DoAs)* each induced by one (centre of DoA) of the four known $\mathcal{SSP}$ parametric distributions denoted as $\mathcal{PD}$ set — *Gamma*, *Inverse Gaussian*, *Log Normal* and *Inverse Gamma*, and representing a range of practically feasible reserve distributions with SC (KCsq) ratio comparable to that of its centre:

- *Gamma DoA* — for modelling reserve risk profiles with relatively low skewness and light tail, i.e. with SC ratio close to 2.0;
- *Inverse-Gaussian (Wald) DoA* — for modelling reserve risk profiles with moderate skewness and tailedness, i.e. with SC ratio close to 3.0;
- *Log-Normal DoA* — for modelling reserve risk profiles with medium to large skewness and heavy-tailedness, i.e. with SC ratio taking values from the range of 3.0 to 3.8;
- *Inverse-Gamma (Vinci) DoA* — for modelling reserve risk profiles with excessively large skewness and heavy-tailedness, i.e. with SC ratio taking values from the range of 3.8 to 6.

All the four $\mathcal{PD}$ induced DoAs together in principle cover a fairly wide range of practically feasible reserve risk profiles with SC ratio ranging from 2 to 6 (e.g., see Salzmann *et al.*, 2012; Guy Carpenter, 2014). It is assumed that any reserve risk profile with volatility CoV, relative skewness SC and relative kurtosis KCsq could be located in the system of CoV-SC (KCsq) coordinates with respect to the $\mathcal{PD}$ parametric distributions — centres of the four DoAs considered. This is the key assumption of reserve risk profile characterisation that is further used in the derivation of PoS approximation formulae in Sections 3 and 4.

TABLE 1

SC AND KCSQ RATIOS FOR THE FOUR PARAMETRIC DISTRIBUTIONS.

$\mathcal{PD}$ Distribution	SC Ratio as a Function of CoV	KCsq Ratio as a Function of CoV^2
Gamma	2	6
Inverse-Gaussian (Wald)	3	15
Log-Normal	$3+\text{CoV}^2 \in (3,4),\ \text{CoV} < 100\%$	$16+15\text{CoV}^2+6\text{CoV}^4+\text{CoV}^6 > 16$
Inverse-Gamma (Vinci)	$\frac{4}{1-\text{CoV}^2} > 4,\ \text{CoV} < 100\%$	$\frac{30(1-\frac{1}{5}\text{CoV}^2)}{(1-\text{CoV}^2)(1-2\text{CoV}^2)} > 30,\ \text{CoV} \leqslant 70\%$

TABLE 2

DIFFERENTIATION OF RESERVE RISK PROFILE BY TYPE OF RESERVE CLASS.

Type of Reserving Class				
Duration	CoV Range	Skewness (SC Ratio)	$\mathcal{PD}$ Induced DoA	Example of Reserving Class
Short Tail	6%–12%	1.9 to 2.1	Gamma	Motor (ex Bodily Injury)
Short Tail	10%–16%	2.0 to 3.0	Gamma, Inverse-Gaussian (Wald)	Home
Short Tail	10%–18%	2.9 to 3.1	Inverse-Gaussian (Wald), Log-Normal	Comm Property/Fire, Comm Accident
Long Tail	12%–25%	3.0 to 3.5	Log-Normal	Motor Bodily Injury, Marine
Long Tail	18%–50%	3.0 to 4.0	Log-Normal, Inverse-Gamma (Vinci)	Workers Comp, Prof Liab, Comm Liab
Long Tail	25%–70%	>4	Inverse-Gamma (Vinci)	Asbestos and Other Long Tail Books

The statistical characteristics of the $\mathcal{PD}$ parametric distributions (centres of the four proposed $\mathcal{PD}$ induced DoAs) are provided in Table 1. Their SC and KCsq ratios are functions of CoV and CoV^2, respectively, and exist for all practically feasible reserve risk profiles, i.e. when CoV $\leqslant 70\%$.

We further use the four $\mathcal{PD}$ induced DoAs to illustrate how reserve risk profiles could be differentiated by type of business/reserving class using CoV and SC. This is presented in Table 2. Here, one would expect that in practice feasible reserve risk profiles have volatility measure CoV in the range of 6% to 70% and relative skewness SC in the range of 2 to 6. These ranges can be supported both directly and indirectly by numerous academic research and empirical studies in reserving (e.g., see Salzmann *et al.*, 2012; Guy Carpenter, 2014).

The graphs of Skewness and Kurtosis as functions of CoV derived from SC and KCsq ratios are provided in Figures 1 and 2. Here, any particular reserve risk profile with skewness $S = \text{SC} \times \text{CoV}$ and kurtosis $K = \text{KCsq} \times \text{CoV}^2$ can be located in the system of CoV-$S(K)$ coordinates with respect to the four $\mathcal{PD}$ parametric distributions. These graphs demonstrate monotonic increase in the level of Skewness and Kurtosis for a given level of CoV when moving sequentially across the $\mathcal{PD}$ set of four proposed parametric distributions from Gamma to Inverse-Gamma.

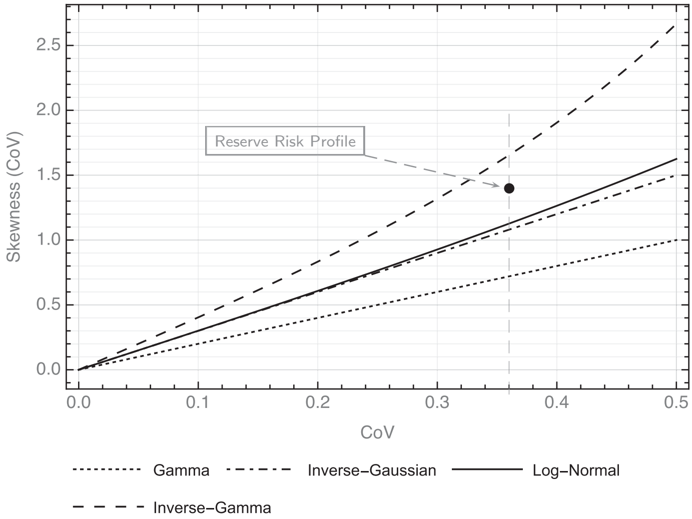

FIGURE 1: Skewness as a function of CoV: reserve risk profile vs. four $\mathcal{PD}$ parametric distributions.

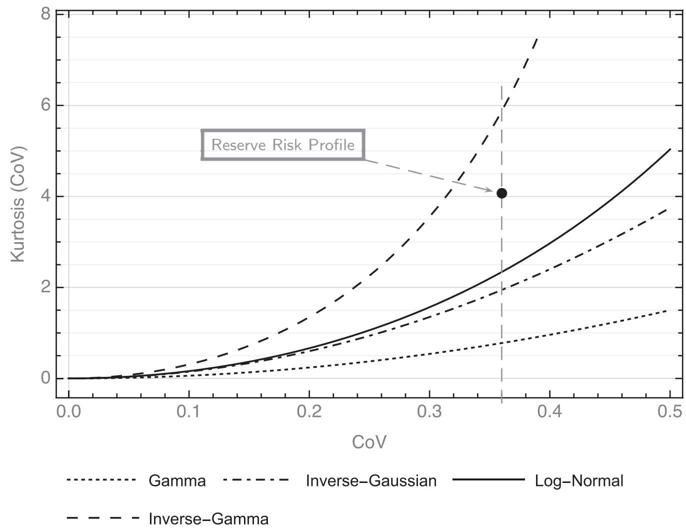

FIGURE 2: Kurtosis as a function of CoV: reserve risk profile vs. four $\mathcal{PD}$ parametric distributions.

Aggregate reserve risk profile. The derivation of the distribution of aggregate risk at the portfolio level is in general not a trivial task and to a large extent is associated with dependence modelling uncertainty. In Embrechts and Jacobsons (2016), the authors studied the lower and upper bounds of the quantile estimate of the aggregate risk distribution and showed how wide the interval estimate

https://doi.org/10.1017/asb.2017.12 Published online by Cambridge University Press

could be when the uncertainty in the choice of the most appropriate dependence structure is taken into account.

Assumption 3. The choice of the most appropriate dependence structure should be determined through the use of adequate calibration process. However, this paper does not focus on the calibration of the most appropriate dependence structure for aggregating reserve risk, but rather assumes that in practice the Gaussian dependence structure is likely to be reasonable, if not the most appropriate one, for aggregating reserve risk, given the confidence levels we are looking at do not include extreme quantiles.

It is also assumed that the matrix of Kendall's tau correlation coefficients, R, is available and used to calibrate the Gaussian copula. This means that the rank correlation (Kendall tau) between classes i and j, $r_{ij} = R(i, j)$, is transformed to the corresponding linear correlation coefficient ρ_{ij} in the following way:

$$\rho_{ij} = \sin\left(\frac{\pi}{2} r_{ij}\right). \tag{5}$$

Assumption 4. It is assumed in this paper that, in practice, any reserve risk profile is characterised sufficiently well by its finite moments of up to the fourth order, i.e. mean (best estimate), CoV, skewness and kurtosis. In particular, the random reserve value, X, can be expressed through its centralised and normalised copy:

$$X = \mathrm{BE}_X \cdot \left(1 + \mathrm{CoV}_X \cdot \widetilde{X}\right), \tag{6}$$

where $\widetilde{X} = \frac{X - \mathrm{BE}_X}{\mathrm{BE}_X \cdot \mathrm{CoV}_X}$ is a non-normal random variable with zero mean and unit standard deviation. The random variable $\widetilde{X}$ is then approximated using the Fleishman approximation:

$$\widetilde{X} = aZ + b(Z^2 - 1) + cZ^3, \quad Z \sim \mathcal{N}(0, 1), \tag{7}$$

where the Fleishman coefficients a, b and c are calibrated by matching the second, third and fourth moments of $\widetilde{X}$ to 1 (standard deviation), γ (skewness) and $\iota + 3$ (absolute or non-centralised kurtosis), respectively. Please note that γ and ι are also skewness and kurtosis of X as they are invariant[12] with respect to translation and scaling. In Section 4, the paper considers two different cases of Fleishman approximation:

1. approximation using skewness only, i.e. $\widetilde{X} = aZ + b(Z^2 - 1)$; and
2. approximation using skewness and kurtosis, i.e. $\widetilde{X} = aZ + b(Z^2 - 1) + cZ^3$.

The calibration of Fleishman coefficients in the first approximation is straightforward and can be analytically expressed, whereas the coefficients of the second approximation are numerically pre-computed and tabulated in the appendices for a given level of CoV and the skewness and kurtosis expressed as functions of CoV.

These are the key assumptions used in the derivation of characteristics of aggregate reserve risk profile outlined in Section 4. The work done in Section 4 could be further extended to other types of copula structures. For example, the recent research work by Gijbels and Herrmann (2014) provides some useful insight into the approximation of distribution of sum of random variables with copula-induced dependence structure. This can be utilised in order to alter the approximation formulae for PoS of risk margin at the aggregate reserve risk level already obtained in Section 4 to allow for the use of other non-Gaussian dependence structures.

2.2. Reserve risk margin and its level of confidence

Risk margin. The risk margin of the non-hedgeable insurance liabilities is similar to what is called *"available solvency margin"* (or capital requirements) under Solvency II. Both represent a form of safety load and are important and necessary to ensure the overall sufficiency of the solvency assessment. However, the role the risk margin plays is quite distinctive from that of "available solvency margin". The risk margin reflects the *uncertainty* in the best estimates of reserves, whereas the actual volatility of reserving process (reserve risk) is fully absorbed by capital requirements. This can be illustrated by decomposing the mean square error of estimating the unknown true unbiased mean of reserves, BE, by its best estimate, $\widehat{\mathrm{BE}}$, provided by a reserving actuary:

$$\begin{aligned}\mathbb{E}\left[\left(\mathrm{BE}-\widehat{\mathrm{BE}}\right)^2\right] &= \mathbb{E}\left[\left(\left(\mathrm{BE}-\mathbb{E}\left[\widehat{\mathrm{BE}}\right]\right)+\left(\mathbb{E}\left[\widehat{\mathrm{BE}}\right]-\widehat{\mathrm{BE}}\right)\right)^2\right] \\ &= \left(\mathrm{BE}-\mathbb{E}\left[\widehat{\mathrm{BE}}\right]\right)^2 + 2\,\mathbb{E}\left[\left(\mathrm{BE}-\mathbb{E}\left[\widehat{\mathrm{BE}}\right]\right)\left(\mathbb{E}\left[\widehat{\mathrm{BE}}\right]-\widehat{\mathrm{BE}}\right)\right] \\ &\quad + \mathbb{E}\left[\left(\mathbb{E}\left[\widehat{\mathrm{BE}}\right]-\widehat{\mathrm{BE}}\right)^2\right] \\ &= \mathrm{bias}^2 + \mathrm{Var}\left[\widehat{\mathrm{BE}}\right] \\ &= \mathrm{bias}^2 + \mathbb{E}\left[\mathrm{Var}\left[\widehat{\mathrm{BE}}\mid\mathcal{F}\right]\right] + \mathrm{Var}\left[\mathbb{E}\left[\widehat{\mathrm{BE}}\mid\mathcal{F}\right]\right], \end{aligned} \tag{8}$$

where bias $= \mathrm{BE} - \mathbb{E}\left[\widehat{\mathrm{BE}}\right]$; $\mathcal{F} = \sigma\left\{\mathbf{M}, \mathbf{BE}\right\}$ is the information filtration (σ-algebra) generated by a set of models **M** and a set of true parameters **BE**. The first term in (8), mean squared bias, is a matter of insurance supervisor's attention and its minimisation is regulated in Pillar II of Solvency II. The second term is the expected variability of reserve risk process, which is fully captured by the Solvency II capital requirements, and the latter term is the volatility of the mean best estimate, which represents the uncertainty in the true best estimate of reserve and the choice of the most appropriate actuarial model. Therefore, this latter term is captured by the risk margin.

The role the risk margin plays in measuring reserve best estimate uncertainty perfectly resonates with the role it plays in the market-consistent valuation of reserves in which the risk-adjusted (market-consistent) expected value of future liability cashflows would implicitly allow for a risk margin.

As was already mentioned in Section 1, the market-consistent value of non-hedgeable liabilities in incomplete insurance markets can be obtained by using either (1) various optimal hedging techniques that minimise the variance of the payoff risk (e.g., see Møller, 2004; Møller and Steffensen, 2007) or, alternatively, (2) a mark-to-model approach under which the liabilities could be transferred to a willing rational counterparty at a price that would fully reflect the market/buyer's perception of risk. The price for assuming risk from insurance liability portfolio transfer comes in the form of an economic risk margin that is explicitly calculated and stacked on top of the best estimate. In this case, the risk margin is equivalent to the current exit value defined by IASB (see IASB, 2007) as *"The amount the insurer would expect to pay at the reporting date to immediately transfer its remaining contractual rights and obligations to another entity"*.

Under the upcoming Solvency II, the prescribed approach to calculating risk margin of non-hedgeable insurance liabilities is the CoC approach. Under the CoC approach, the margin for uncertainty in liability valuation is directly linked to the market price for assuming reserve risk from insurance liability portfolio transfer by a willing third party (cf. Strommen, 2006). This market price is measured by the cost of regulatory capital required to runoff all liabilities. Exactly in such a context the CoC approach was first introduced in the Swiss Solvency Test (SST) in 2004 (cf. SST, 2004; SCOR, 2008; Sandström, 2011). The derivation of CoC risk margin entails (for details please refer to Sandström, 2011):

- projecting the Solvency Capital Requirements (SCR) net of diversification benefits for non-hedgeable risks from time $t = 1$ to full runoff;
- calculating the capital charge at the end of each projection year by multiplying SCR_t by the CoC charge c_t; and
- taking the total present value of projected capital charges to determine the overall CoC risk margin.

Assumption 5. It is not the aim of this paper to provide the derivation of the CoC risk margin as it is assumed here that it is pre-calculated and provided by reserving and/or capital actuaries at both single class level and the portfolio level. The CoC risk margins are assumed to be expressed as a percentage of reserve best estimate BE and denoted by

- η_i — relative risk margin for ith standalone reserving class expressed as a percentage of ith class's best estimate BE_i; and

https://doi.org/10.1017/asb.2017.12 Published online by Cambridge University Press

- η_Σ — relative risk margin for the portfolio of multiple reserving classes expressed as a percentage of portfolio's best estimate BE_Σ.

In practice, the relative risk margin of booked technical provisions does not exceed 30% (e.g., see IAA, 2009). We use this as an assumption of practical feasibility of η throughout the paper.

Level of confidence: measurement and approximation. The IFRS level of confidence of the Solvency II risk margin is measured by PoS. For a given random reserve value X with best estimate BE_X, level of variability CoV_X and risk margin η_X the PoS is defined as

$$\text{PoS} = \mathbb{P}[X \leqslant \text{BE}_X \cdot (1 + \eta_X)] = \alpha. \tag{9}$$

To solve for unknown level of PoS, α, one would need first to invert PoS by taking Value at Risk (VaR) of X at α

$$\text{VaR}_\alpha(X) = \text{BE}_X \cdot (1 + \eta_X)\,, \tag{10}$$

and then express $\text{VaR}_\alpha(X)$ through the VaR of centralised and normalised copy of X, $\widetilde{X} = \frac{X - \text{BE}_X}{\text{BE}_X \cdot \text{CoV}_X}$, and solve the following equation for α

$$\text{BE}_X \cdot \left(1 + \text{CoV}_X \cdot \text{VaR}_\alpha\left(\widetilde{X}\right)\right) = \text{BE}_X \cdot (1 + \eta_X)\,, \tag{11}$$

or equivalently the equation

$$\text{VaR}_\alpha\left(\widetilde{X}\right) = \frac{\eta_X}{\text{CoV}_X}. \tag{12}$$

It should be noted that the linearity of VaR transformation used in equation (11) holds for any distribution.

The (12) indicates that the level of PoS is dependent only on the relative risk margin η_X (the risk margin per unit of BE_X) and the level of variability of X measured by CoV_X, and thus is invariant with respect to BE_X — the location of the risk profile of X.

Assumption 6. To solve for PoS level, α, this paper suggests inverting (12) by using the following approximations:

1. the C-F approximation of $\text{VaR}_\alpha\left(\widetilde{X}\right)$ derived from the C-F expansion series[13] of the quantiles of the random variable X via its finite cumulants[14]

https://doi.org/10.1017/asb.2017.12 Published online by Cambridge University Press

and the standard normal quantiles:

$$\begin{aligned}\mathrm{VaR}_\alpha(\widetilde{X}) \approx\; & z_\alpha + \gamma_X \frac{z_\alpha^2 - 1}{6} \\ & + C_1 \left(\iota_X \frac{z_\alpha^3 - 3z_\alpha}{24} - \gamma_X^2 \frac{2z_\alpha^3 - 5z_\alpha}{36} \right) \\ & + C_2 \left(-\gamma_X \iota_X \frac{z_\alpha^4 - 5z_\alpha^2 + 2}{24} + \gamma_X^3 \frac{12z_\alpha^4 - 53z_\alpha^2 + 17}{324} \right),\end{aligned} \tag{13}$$

where the coefficients C_1 and C_2 are binary switches and take values from $\{0, 1\}$ defining the following specific cases of C-F approximation:

- $C_1 = C_2 = 0$ – second-order Cornish-Fisher (or, equivalently, first-order Normal Power) approximation utilising only skewness γ_X of X;
- $C_1 = 1$ and $C_2 = 0$ — third-order C-F (or, equivalently, second-order Normal Power) approximation utilising skewness γ_X and kurtosis ι_X of X; and
- $C_1 = C_2 = 1$ — fourth-order C-F approximation utilising skewness γ_X and kurtosis ι_X of X;

here, the PoS level, α, is recovered by solving a C-F polynomial equation for standard normal quantile z_α and mapping it to $\alpha = \Phi(z_\alpha)$; and

2. the B-E approximation of PoS level, α, in the form of an inversion $\mathrm{VaR}_\alpha\left(\widetilde{X}\right) \mapsto \alpha$ using the incomplete Gamma function

$$\alpha \approx \frac{1}{\Gamma(s)} \int_0^{s+\sqrt{s}\,q} y^{s-1} e^{-y}\, dy, \tag{14}$$

where $q = \mathrm{VaR}_\alpha\left(\widetilde{X}\right) = \frac{\eta_X}{\mathrm{CoV}_X}$ and $s = \frac{4}{\gamma_X^2}$, which is equivalent to using a Gamma distribution $F_Y(y)$ with $Y \sim \mathrm{Gamma}(s, 1)$ evaluated at $y = s + \sqrt{s}\,q$.

We denote the set of the proposed PoS approximations above by $\mathcal{A}$ and will use this notation throughout the paper.

The above approximations were proposed mainly for their ability to estimate the reserve distribution quantiles using relative moments of the reserve distribution — i.e. the reserve risk characteristics that may often be available at hand to reserving actuaries, and that what makes them attractive from the practical point of view. However, in general, when it comes to estimating VaR, these are not the only methods of distribution quantile approximation available, there are also other alternatives. Below lists these alternatives briefly outlining their features and explaining why they were not chosen in this paper.

- The *Haldane method* (see Haldane, 1938; Pentikäinen, 1987) and the Wilson–Hilferty method (see Wilson and Hilferty, 1931; Pentikäinen, 1987) — used to

https://doi.org/10.1017/asb.2017.12 Published online by Cambridge University Press

approximate the distribution quantile using CoV and skewness of the distribution. These approximation methods are based on (a) *Symmetrisation* and (b) *Normal Approximation* — here (a) transforms a random variable into a symmetric random variable, and (b) then applies Normal approximation to it. It should be noted that the C-F approximations are also based on using symmetrisation and Normal approximation. As was shown in Daykin *et al.* (1994), these two methods are as good as Normal Power approximation (i.e. second order C-F approximations) for a reasonable wide range of quantiles and all practically feasible values of skewness. However, like for Normal Power, their quality of approximation for a fairly high quantiles in the tail of distribution would rapidly deteriorate when skewness exceeds unity, or at most the value 1.2. Given that, it was decided to go with more known C-F approximation.

- The *GPD method* — used to approximate the distribution quantiles above a certain threshold. This approximation is based on the result from the Extreme Value Theory (see Christoffersen, 2011; Embrechts *et al.*, 2011; Embrechts *et al.*, 2015), which states that for a large enough threshold the distribution of excess losses above the threshold can be approximated by a Generalised Pareto Distribution (GPD). This method is sensible and reliable when applied to estimating high quantile values only up in the tail of the distribution — in practice, it would be applied to quantiles with the return period of at least 1-in-20 years. On the other hand, reserve technical provisions are booked at the level between 50th and 90th, or 95th percentile at most, making it difficult to reliably apply the GPD method to estimating the PoS level of the reserve risk margin.
- The *Hill method* — an alternative to the GPD method used to estimate high quantiles up in the tail of the distribution. Like in the case of the GPD method, it is reliable when applied to estimating quantiles above a large enough threshold, but also additionally assumes that the tail of the distribution above the chosen threshold is a regularly varying (or a power-law) function (see Christoffersen, 2011; Embrechts *et al.*, 2011, 2015). Again, it is the choice of a fairly high threshold (i.e. above 95th percentile) required for this method to be sensible that prevents it from being suitable for estimating PoS levels of the reserve risk margin, or, equivalently, effective probability percentages of the reserve technical provisions booked, which in practice do not exceed 95%.

Obviously, the chosen approximations are not without drawbacks. For example, the main known shortcoming of the C-F approximation is that its quality deteriorates as one moves to extreme quantile values up in the tail of the distribution and/or when the distribution becomes excessively skewed and/or leptokurtic (e.g., see Kotz *et al.*, 1994; Christoffersen, 2011). One thing that assures the applicability of the C-F approximations to estimating PoS levels in reserving is that in reality the reserve technical provisions are generally booked at the level ranging from 50th to 90th percentile. It is the non-extreme nature of these percentiles that provides such assurance. However, there is still a chance that it may not be as ideal as one would wish in the case when dealing with excessively skewed/leptokurtic reserve risk profiles, hence raising the question about its quality, and this is what we would like to test in this paper. With respect to the B-E approximation developed by Bohman and Esscher in their 1963–1964 seminal papers Bohman and Esscher (1963) and Bohman and Esscher (1964), it is somewhat more promising, as, according to Seal (1977), it is superior to the C-F approximations of second and third order (as per our definition of the C-F approximation above), and its quality is not impacted by the level of skewness.

3. PoS APPROXIMATIONS AND THEIR QUALITY - STANDALONE RESERVING CLASS

This section focuses on the following two things:

- providing explicit analytical formulae for the four proposed approximations of PoS level of reserve risk margin of a standalone reserving class; and
- analysing their quality.

Since the B-E approximation is the only approximation that explicitly defines the PoS estimate, our focus is then on providing explicit formula for estimating PoS level with the three C-F approximations:

1. *"C-F Quadratic"* — second-order C-F (or first-order Normal Power) approximation;
2. *"C-F Cubic"* — third-order C-F (or second-order Normal Power) approximation; and
3. *"C-F Quartic"* — fourth-order C-F approximation.

This is done in Sections 3.1–3.3. The quality of obtained C-F approximations along with the B-E approximation is then analysed in Section 3.4.

3.1. First-order normal power approximation (C_1=C_2=0)

The first-order Normal Power approximation of $\mathrm{VaR}_\alpha\left(\widetilde{X}\right)$ utilises only skewness γ_X of X:

$$\mathrm{VaR}_\alpha(\widetilde{X}) \approx z_\alpha + \gamma_X \frac{z_\alpha^2 - 1}{6}. \tag{15}$$

Let $q = \frac{\eta_X}{\mathrm{CoV}_X}$. Then, to find unknown z_α, we solve the quadratic equation

$$z_\alpha + \gamma_X \frac{z_\alpha^2 - 1}{6} = q, \quad \text{or equivalently}$$

$$z_\alpha^2 + \frac{6}{\gamma_X} z_\alpha - \left(\frac{6}{\gamma_X} q + 1\right) = 0. \tag{16}$$

https://doi.org/10.1017/asb.2017.12 Published online by Cambridge University Press

There is only one real positive root of the quadratic equation (16) and it is equal to

$$\widehat{z}_\alpha = -\frac{3}{\gamma_X} + \sqrt{\frac{9}{\gamma_X^2} + \frac{6}{\gamma_X} q + 1}. \tag{17}$$

The PoS level, α, is then found as follows

$$\widehat{\alpha} = \Phi(\widehat{z}_\alpha). \tag{18}$$

3.2. Second-order Normal Power approximation (C_1=1, C_2=0)

The second-order Normal Power approximation of $\mathrm{VaR}_\alpha\left(\widetilde{X}\right)$ utilises both skewness γ_X and kurtosis ι_X of X:

$$\mathrm{VaR}_\alpha(\widetilde{X}) \approx z_\alpha + \gamma_X \frac{z_\alpha^2 - 1}{6} + \iota_X \frac{z_\alpha^3 - 3z_\alpha}{24} - \gamma_X^2 \frac{2z_\alpha^3 - 5z_\alpha}{36}. \tag{19}$$

To find unknown z_α, we solve the following cubic equation

$$z_\alpha + \gamma_X \frac{z_\alpha^2 - 1}{6} + \iota_X \frac{z_\alpha^3 - 3z_\alpha}{24} - \gamma_X^2 \frac{2z_\alpha^3 - 5z_\alpha}{36} = q,$$

or equivalently

$$a z_\alpha^3 + b z_\alpha^2 + c z_\alpha + d = 0, \tag{20}$$

where

$$\begin{cases} a = \frac{1}{24}\iota_X - \frac{1}{18}\gamma_X^2, \\ b = \frac{1}{6}\gamma_X, \\ c = 1 + \frac{5}{36}\gamma_X^2 - \frac{1}{8}\iota_X, \\ d = -\frac{1}{6}\gamma_X - q. \end{cases} \tag{21}$$

The roots of the cubic equation (20) can be found using the Cardano's formula (see, e.g., Abramowitz and Stegun, 1972)

$$\begin{cases} x_1 = M + N - \frac{b}{3a}, \\ x_2 = -\frac{M+N}{2} - \frac{b}{3a} + \frac{i\sqrt{3}}{2}(M - N), \\ x_3 = -\frac{M+N}{2} - \frac{b}{3a} - \frac{i\sqrt{3}}{2}(M - N), \end{cases} \tag{22}$$

https://doi.org/10.1017/asb.2017.12 Published online by Cambridge University Press

where

$$M = \sqrt[3]{P + \sqrt{P^2 + Q^3}}, \tag{23}$$

$$N = \sqrt[3]{P - \sqrt{P^2 + Q^3}}, \tag{24}$$

where

$$P = \frac{9abc - 27a^2d - 2b^3}{54a^3}, \tag{25}$$

$$Q = \frac{3ac - b^2}{9a^2}. \tag{26}$$

The existence of real roots of the cubic equation (20) and their quantity are dependent on the sign of cubic discriminant

$$D = P^2 + Q^3. \tag{27}$$

We consider three cases of D:

1. if $D > 0$, then there exists only one real root and it is equal to $M + N - \frac{b}{3a}$;
2. if $D = 0$, then all three roots are real, and at least two are the same and equal to $-\frac{M+N}{2} - \frac{b}{3a}$; and
3. if $D < 0$, then all three roots are real and unequal.

In the latter case, when $D < 0$, the three real roots can also be expressed trigonometrically:

$$\begin{cases} x_1 = 2\sqrt{-Q}\cos\left(\frac{\varphi}{3}\right) - \frac{b}{3a}, \\ x_2 = 2\sqrt{-Q}\cos\left(\frac{\varphi}{3} + \frac{2\pi}{3}\right) - \frac{b}{3a}, \\ x_3 = 2\sqrt{-Q}\cos\left(\frac{\varphi}{3} + \frac{4\pi}{3}\right) - \frac{b}{3a}, \end{cases} \tag{28}$$

where $\varphi = \arccos(\frac{P}{\sqrt{-Q^3}})$.

In any case, the root $\widehat{z}_\alpha$ is then the largest of all real roots of the cubic equation (20). The PoS level, α, is then found as follows

$$\widehat{\alpha} = \Phi(\widehat{z}_\alpha). \tag{29}$$

The functional analysis of the roots of the cubic equation (20) can be done by analysing its discriminant D. As was assumed earlier in Section 2, both skewness and kurtosis are functionally related to the CoV of the random variable X. In particular, these functional relations will take a certain form as the distribution of X is assumed to be adhered to one of the four types of parametric distributions defined in Section 2. By taking this into account, we conclude that the discriminant D is simply an analytical function of the coefficient of variation CoV_X and the relative risk margin η_X. The function $D\,(\mathrm{CoV}_X, \eta_X)$ is analysed

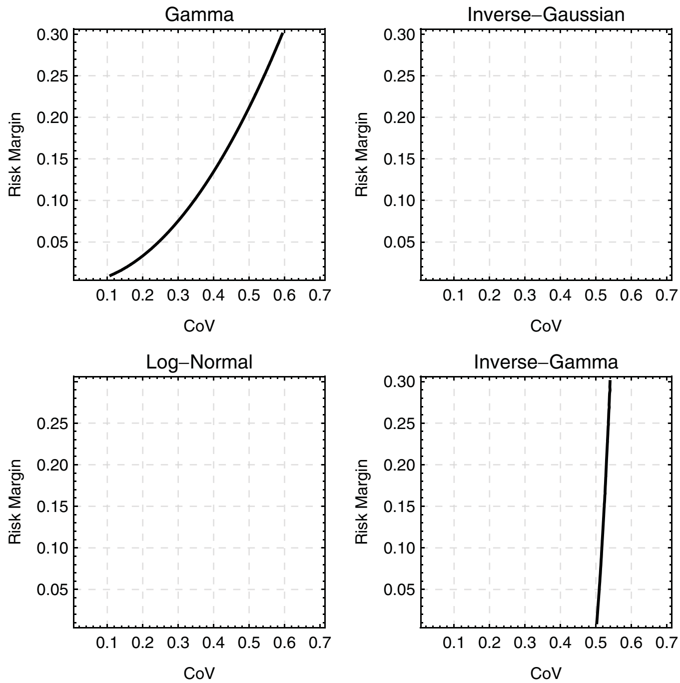

FIGURE 3: Contour graph of the discriminant D.

on the range of feasible/practical values of CoV_X and η_X:

$$\mathcal{R} = \{(\text{CoV}_X, \eta_X) \mid 0\% \leqslant \text{CoV}_X \leqslant 70\%\,,\ 0\% \leqslant \eta_X \leqslant 30\%\}\,.$$

The Figure 3 depicts the contour graph of D surface for each of the four parametric distributions from $\mathcal{PD}$. The discriminant D changes its sign from positive to negative at the contour graph when moving from left to right. This is the case for Gamma and Inverse-Gamma distributions, although for most practical situations — CoV $< 20\%$ and $\eta > 5\%$ for Gamma, and CoV $< 50\%$ for Inverse-Gamma, the discriminant D has a positive value. The contour graph for Inverse-Gaussian and Log-Normal distributions is empty, indicating that D on $\mathcal{R}$ is positive and hence there exists only one real root of cubic approximation.

3.3. Fourth-order Cornish–Fisher approximation ($C_1 = C_2 = 1$)

The fourth-order C-F approximation of $\text{VaR}_\alpha\left(\widetilde{X}\right)$ utilises both skewness γ_X and kurtosis ι_X of X and in addition to the terms of the second-order Normal Power

https://doi.org/10.1017/asb.2017.12 Published online by Cambridge University Press

approximation (19) involves terms containing z_α^4:

$$\begin{aligned}\mathrm{VaR}_\alpha(\widetilde{X}) \approx z_\alpha + \gamma_X\frac{z_\alpha^2-1}{6} + \iota_X\frac{z_\alpha^3-3z_\alpha}{24}\\ - \gamma_X^2\frac{2z_\alpha^3-5z_\alpha}{36} - \gamma_X\iota_X\frac{z_\alpha^4-5z_\alpha^2+2}{24}\\ + \gamma_X^3\frac{12z_\alpha^4-53z_\alpha^2+17}{324}.\end{aligned} \tag{30}$$

To find unknown z_α, we solve the following quartic equation

$$\begin{aligned}q = z_\alpha + \gamma_X\frac{z_\alpha^2-1}{6} + \iota_X\frac{z_\alpha^3-3z_\alpha}{24}\\ - \gamma_X^2\frac{2z_\alpha^3-5z_\alpha}{36} - \gamma_X\iota_X\frac{z_\alpha^4-5z_\alpha^2+2}{24}\\ + \gamma_X^3\frac{12z_\alpha^4-53z_\alpha^2+17}{324},\end{aligned}$$

or equivalently

$$a z_\alpha^4 + b z_\alpha^3 + c z_\alpha^2 + d z_\alpha + e = 0, \tag{31}$$

where

$$\begin{cases} a = \frac{1}{27}\gamma_X^3 - \frac{1}{24}\gamma_X\iota_X, \\ b = \frac{1}{24}\iota_X - \frac{1}{18}\gamma_X^2, \\ c = \frac{1}{6}\gamma_X + \frac{5}{24}\gamma_X\iota_X - \frac{53}{324}\gamma_X^3, \\ d = 1 + \frac{5}{36}\gamma_X^2 - \frac{1}{8}\iota_X, \\ e = -\frac{1}{6}\gamma_X + \frac{17}{324}\gamma_X^3 - \frac{1}{12}\gamma_X\iota_X - q. \end{cases} \tag{32}$$

The roots of the quartic equation (31) can be found using the Ferrari's method (see, e.g., Abramowitz and Stegun, 1972, or for the detailed description of a unifying approach to solving quartic equations please refer to Shmakov, 2011):

$$x = \frac{-p \pm \sqrt{p^2-8t}}{4}, \tag{33}$$

where

$$p = \frac{b}{a} \pm \sqrt{\frac{b^2}{a^2} - \frac{4c}{a} + 4y}, \tag{34}$$

$$t = y \mp \sqrt{y^2 - \frac{4e}{a}}, \tag{35}$$

https://doi.org/10.1017/asb.2017.12 Published online by Cambridge University Press

where y is the largest root of the cubic resolvent

$$y^3 - \frac{c}{a}y^2 + \left(\frac{bd}{a^2} - \frac{4e}{a}\right)y + \left(\frac{4ce}{a^2} - \frac{b^2e}{a^3} - \frac{d^2}{a^2}\right) = 0. \tag{36}$$

The root $\widehat{z}_\alpha$ is then the largest of all real roots of the quartic equation (31) from (0, 1). The PoS level, α, is then found as follows:

$$\widehat{\alpha} = \Phi(\widehat{z}_\alpha). \tag{37}$$

3.4. Analysis of quality of approximations

This subsection provides the analysis of the quality of the four types of PoS approximations proposed. Specifically, the analysis was performed using numerical computations and comparing each type of PoS approximation to the theoretical value of PoS derived from a given parametric distribution from $\mathcal{PD}$.

Given the parametric distribution (CDF) $F_{u,v} \in \mathcal{PD}$[15] and the PoS approximation $A \in \mathcal{A}$,[16] the following comparison is made for each pair of coefficient of variation CoV and risk margin η from the range $\mathcal{R}' = \{(\mathrm{CoV}, \eta) \mid 0\% \leqslant \mathrm{CoV} \leqslant 50\%, \quad 0\% \leqslant \eta \leqslant 30\%\} \subset \mathcal{R}$:

$$\widehat{\mathrm{PoS}}_A \text{ vs. } \mathrm{PoS}_F = F_{u',v}(1+\eta),$$

where $F_{u',v}$ is assumed to be normalised so that its mean is one and standard deviation is CoV, and thus the scale parameter u' is a function of shape parameter v (as per (2) and the explanations provided on page 742). To compute $F_{u',v}(1+\eta)$, the following analytical formulae were used:

- *Inverse-Gaussian* distribution
  - ▷ $X \sim \mathrm{IG}\left(\frac{\nu}{\theta}, \frac{\nu^2}{\theta}\right)$ with cumulative distribution function $F_{\theta,\nu}(x) = \Phi\left(\frac{\theta x - \nu}{\sqrt{\theta x}}\right) + e^{2\nu}\,\Phi\left(-\frac{\theta x + \nu}{\sqrt{\theta x}}\right)$;
  - ▷ $\nu = \frac{1}{\mathrm{CoV}^2}$;
  - ▷ $\theta'(\nu) = \nu$;
- *Log-Normal* distribution
  - ▷ $X \sim \mathrm{LN}(\mu, \sigma) = \Phi\left(\frac{\ln x - \mu}{\sigma}\right)$ with cumulative distribution function $F_{\mu,\sigma}(x)$;
  - ▷ $\sigma^2 = \ln\left(\mathrm{CoV}^2 + 1\right)$;
  - ▷ $\mu'(\sigma) = -\frac{1}{2}\sigma^2$;
- *Gamma* distribution
  - ▷ $X \sim \mathrm{Gamma}(\alpha, \beta)$ with cumulative distribution function $F_{\beta,\alpha}(x) = \frac{\Gamma(\alpha) - \Gamma\left(\alpha, \frac{x}{\beta}\right)}{\Gamma(\alpha)}$;
  - ▷ $\alpha = \frac{1}{\mathrm{CoV}^2}$;
  - ▷ $\beta'(\alpha) = \frac{1}{\alpha}$;

https://doi.org/10.1017/asb.2017.12 Published online by Cambridge University Press

- *Inverse-Gamma* distribution
  - ▹ $X \sim \text{InvGamma}(\alpha, \beta)$ with cumulative distribution function $F_{\beta,\alpha}(x) = \frac{\Gamma(\alpha, \frac{\beta}{x})}{\Gamma(\alpha)}$;
  - ▹ $\alpha = \frac{1}{\text{CoV}^2} + 2$;
  - ▹ $\beta'(\alpha) = \alpha - 1$;
  - ▹ $F_{\beta,\alpha}(x) = 1 - CDF_Y\left(\frac{1}{x}\right)$, where $Y \sim \text{Gamma}\left(\alpha, \frac{1}{\beta}\right)$.

The results of the analysis are provided in the following four subsections. There, $\Delta\%$ error of PoS approximation $\mathcal{A}$ is defined as

$$\Delta\% = \frac{\text{PoS}_F - \widehat{\text{PoS}}_A}{\widehat{\text{PoS}}_A} \cdot 100\%.$$

The quality of the four approximations in scope is analysed[17] with reference to the absolute value of their corresponding relative error, $|\Delta|\,\%$. In particular, the approximations have been ranked in ascending order of $|\Delta|\,\%$ values, and also highlighted/labelled in such a way that when ranked it is also visible to which of the following four bands of adherence quality each approximation belongs to:

- band 1: $|\Delta| \leqslant 1\%$;
- band 2: $1\% < |\Delta| \leqslant 2.5\%$;
- band 3: $2.5\% < |\Delta| \leqslant 5\%$; and
- band 4: $|\Delta| > 5\%$.

Specifically, each approximation name would be highlighted in a specific colour and have a bracketed number attached to it indicating what band of adherence quality it belongs to. The following table provides the mapping of colour keys and bracketed numbers to the four bands as used in Tables 3, 4, 5, and 6:

Band	Bracketed Number	Colour Key
$\lvert\Delta\rvert \leqslant 1\%$	1	
$1\% < \lvert\Delta\rvert \leqslant 2.5\%$	2	
$2.5\% < \lvert\Delta\rvert \leqslant 5\%$	3	
$\lvert\Delta\rvert > 5\%$	4	

3.4.1. *Summary of analysis results.* The results (see Tables 3, 4, 5, and 6) of the analysis of quality of the four proposed PoS approximations show that across the whole range of parametric distributions from $\mathcal{PD}$ in most cases the B-E approximation is at least at par with, if not superior to, any of the three C-F approximations. In particular, in such cases it would be either "the best approximation", or if not "the best", then still falling into the band of highest adherence quality (i.e. band 1). However, there are a few situations — exactly 17 out of 240 analysed cases where the B-E approximation, whilst neither being "the best" nor

https://doi.org/10.1017/asb.2017.12 Published online by Cambridge University Press

TABLE 3

ANALYSIS OF QUALITY OF APPROXIMATIONS: SUMMARY RESULTS FOR ESTIMATING GAMMA DISTRIBUTION.

	$\eta = 5\%$				$\eta = 5\%$			
CoV	Best	2nd Best	3rd Best	4th Best	Best	2nd Best	3rd Best	4th Best
5%	B-E[1]	C-F Cubic[1]	C-F Quartic[1]	C-F Quadr[1]	B-E[1]	C-F Cubic[1]	C-F Quartic[1]	C-F Quadr[1]
10%	B-E[1]	C-F Cubic[1]	C-F Quartic[1]	C-F Quadr[1]	B-E[1]	C-F Cubic[1]	C-F Quartic[1]	C-F Quadr[1]
15%	B-E[1]	C-F Cubic[1]	C-F Quartic[1]	C-F Quadr[1]	B-E[1]	C-F Cubic[1]	C-F Quartic[1]	C-F Quadr[1]
20%	B-E[1]	C-F Cubic[1]	C-F Quadr[1]	C-F Quartic[1]	B-E[1]	C-F Cubic[1]	C-F Quartic[1]	C-F Quadr[1]
25%	B-E[1]	C-F Cubic[1]	C-F Quadr[1]	C-F Quartic[1]	B-E[1]	C-F Cubic[1]	C-F Quadr[1]	C-F Quartic[1]
30%	B-E[1]	C-F Cubic[1]	C-F Quadr[1]	C-F Quartic[1]	B-E[1]	C-F Cubic[1]	C-F Quadr[1]	C-F Quartic[1]
35%	B-E[1]	C-F Cubic[1]	C-F Quadr[1]	C-F Quartic[2]	B-E[1]	C-F Cubic[1]	C-F Quadr[1]	C-F Quartic[1]
40%	B-E[1]	C-F Cubic[1]	C-F Quadr[1]	C-F Quartic[2]	B-E[1]	C-F Cubic[1]	C-F Quadr[1]	C-F Quartic[2]
45%	B-E[1]	C-F Cubic[1]	C-F Quadr[1]	C-F Quartic[3]	B-E[1]	C-F Cubic[1]	C-F Quadr[1]	C-F Quartic[2]
50%	B-E[1]	C-F Cubic[1]	C-F Quadr[1]	C-F Quartic[3]	B-E[1]	C-F Cubic[1]	C-F Quadr[1]	C-F Quartic[3]

	$\eta = 15\%$				$\eta = 20\%$			
CoV	Best	2nd Best	3rd Best	4th Best	Best	2nd Best	3rd Best	4th Best
5%	B-E[1]	C-F Cubic[1]	C-F Quadr[1]	C-F Quartic[1]	B-E[1]	C-F Cubic[1]	C-F Quadr[1]	C-F Quartic[1]
10%	B-E[1]	C-F Cubic[1]	C-F Quartic[1]	C-F Quadr[1]	B-E[1]	C-F Cubic[1]	C-F Quartic[1]	C-F Quadr[1]
15%	B-E[1]	C-F Cubic[1]	C-F Quartic[1]	C-F Quadr[1]	B-E[1]	C-F Cubic[1]	C-F Quartic[1]	C-F Quadr[1]
20%	B-E[1]	C-F Cubic[1]	C-F Quartic[1]	C-F Quadr[1]	B-E[1]	C-F Cubic[1]	C-F Quartic[1]	C-F Quadr[1]
25%	B-E[1]	C-F Cubic[1]	C-F Quartic[1]	C-F Quadr[1]	B-E[1]	C-F Cubic[1]	C-F Quartic[1]	C-F Quadr[1]
30%	B-E[1]	C-F Cubic[1]	C-F Quartic[1]	C-F Quadr[1]	B-E[1]	C-F Cubic[1]	C-F Quartic[1]	C-F Quadr[1]
35%	B-E[1]	C-F Cubic[1]	C-F Quadr[1]	C-F Quartic[1]	B-E[1]	C-F Cubic[1]	C-F Quartic[1]	C-F Quadr[1]
40%	B-E[1]	C-F Cubic[1]	C-F Quadr[1]	C-F Quartic[1]	B-E[1]	C-F Cubic[1]	C-F Quartic[1]	C-F Quadr[1]
45%	B-E[1]	C-F Cubic[1]	C-F Quadr[1]	C-F Quartic[2]	B-E[1]	C-F Cubic[1]	C-F Quartic[1]	C-F Quadr[1]
50%	B-E[1]	C-F Cubic[1]	C-F Quadr[1]	C-F Quartic[2]	B-E[1]	C-F Cubic[1]	C-F Quadr[1]	C-F Quartic[2]

https://doi.org/10.1017/asb.2017.12 Published online by Cambridge University Press

TABLE 3

CONTINUED.

	$\eta = 25\%$				$\eta = 30\%$			
CoV	Best	2nd Best	3rd Best	4th Best	Best	2nd Best	3rd Best	4th Best
5%	B-E[1]	C-F Cubic[1]	C-F Quadr[1]	C-F Quartic[1]	B-E[1]	C-F Cubic[1]	C-F Quadr[1]	C-F Quartic[1]
10%	B-E[1]	C-F Quartic[1]	C-F Cubic[1]	C-F Quadr[1]	B-E[1]	C-F Cubic[1]	C-F Quadr[1]	C-F Quartic[1]
15%	B-E[1]	C-F Cubic[1]	C-F Quartic[1]	C-F Quadr[1]	B-E[1]	C-F Cubic[1]	C-F Quartic[1]	C-F Quadr[1]
20%	B-E[1]	C-F Cubic[1]	C-F Quartic[1]	C-F Quadr[1]	B-E[1]	C-F Cubic[1]	C-F Quadr[1]	C-F Quartic[1]
25%	B-E[1]	C-F Cubic[1]	C-F Quartic[1]	C-F Quadr[1]	B-E[1]	C-F Cubic[1]	C-F Quartic[1]	C-F Quadr[1]
30%	B-E[1]	C-F Cubic[1]	C-F Quartic[1]	C-F Quadr[1]	B-E[1]	C-F Cubic[1]	C-F Quartic[1]	C-F Quadr[1]
35%	B-E[1]	C-F Cubic[1]	C-F Quartic[1]	C-F Quadr[1]	B-E[1]	C-F Cubic[1]	C-F Quartic[1]	C-F Quadr[1]
40%	B-E[1]	C-F Cubic[1]	C-F Quartic[1]	C-F Quadr[1]	B-E[1]	C-F Cubic[1]	C-F Quartic[1]	C-F Quadr[1]
45%	B-E[1]	C-F Cubic[1]	C-F Quartic[1]	C-F Quadr[1]	B-E[1]	C-F Cubic[1]	C-F Quartic[1]	C-F Quadr[1]
50%	B-E[1]	C-F Cubic[1]	C-F Quartic[1]	C-F Quadr[2]	B-E[1]	C-F Cubic[1]	C-F Quartic[1]	C-F Quadr[2]

TABLE 4

ANALYSIS OF QUALITY OF APPROXIMATIONS: SUMMARY RESULTS FOR ESTIMATING INVERSE-GAUSSIAN DISTRIBUTION.

	$\eta = 5\%$				$\eta = 10\%$			
CoV	Best	2nd Best	3rd Best	4th Best	Best	2nd Best	3rd Best	4th Best
5%	C-F Cubic[1]	C-F Quartic[1]	B-E[1]	C-F Quadr[1]	C-F Cubic[1]	B-E[1]	C-F Quartic[1]	C-F Quadr[1]
10%	C-F Cubic[1]	B-E[1]	C-F Quartic[1]	C-F Quadr[1]	C-F Cubic[1]	B-E[1]	C-F Quartic[1]	C-F Quadr[1]
15%	C-F Cubic[1]	B-E[1]	C-F Quadr[1]	C-F Quartic[1]	C-F Cubic[1]	C-F Quartic[1]	B-E[1]	C-F Quadr[1]
20%	B-E[1]	C-F Cubic[1]	C-F Quadr[1]	C-F Quartic[1]	C-F Cubic[1]	B-E[1]	C-F Quartic[1]	C-F Quadr[1]
25%	B-E[1]	C-F Cubic[1]	C-F Quadr[1]	C-F Quartic[2]	B-E[1]	C-F Cubic[1]	C-F Quadr[1]	C-F Quartic[1]
30%	B-E[1]	C-F Cubic[1]	C-F Quadr[1]	C-F Quartic[3]	B-E[1]	C-F Cubic[1]	C-F Quadr[1]	C-F Quartic[2]
35%	B-E[1]	C-F Quadr[1]	C-F Cubic[1]	C-F Quartic[3]	B-E[1]	C-F Cubic[1]	C-F Quadr[2]	C-F Quartic[3]
40%	B-E[1]	C-F Quadr[1]	C-F Cubic[2]	C-F Quartic[4]	B-E[1]	C-F Cubic[1]	C-F Quadr[2]	C-F Quartic[3]
45%	B-E[1]	C-F Quadr[1]	C-F Cubic[2]	C-F Quartic[4]	B-E[1]	C-F Cubic[2]	C-F Quadr[2]	C-F Quartic[4]
50%	B-E[1]	C-F Quadr[1]	C-F Cubic[2]	C-F Quartic[4]	B-E[1]	C-F Quadr[2]	C-F Cubic[2]	C-F Quartic[4]

	$\eta = 15\%$				$\eta = 20\%$			
CoV	Best	2nd Best	3rd Best	4th Best	Best	2nd Best	3rd Best	4th Best
5%	C-F Cubic[1]	C-F Quartic[1]	B-E[1]	C-F Quadr[1]	C-F Cubic[1]	B-E[1]	C-F Quadr[1]	C-F Quartic[1]
10%	C-F Cubic[1]	B-E[1]	C-F Quartic[1]	C-F Quadr[1]	B-E[1]	C-F Cubic[1]	C-F Quadr[1]	C-F Quartic[1]
15%	C-F Cubic[1]	B-E[1]	C-F Quartic[1]	C-F Quadr[1]	C-F Cubic[1]	B-E[1]	C-F Quartic[1]	C-F Quadr[1]
20%	C-F Cubic[1]	C-F Quartic[1]	B-E[1]	C-F Quadr[1]	C-F Cubic[1]	B-E[1]	C-F Quartic[1]	C-F Quadr[1]
25%	C-F Cubic[1]	B-E[1]	C-F Quartic[1]	C-F Quadr[1]	C-F Cubic[1]	B-E[1]	C-F Quartic[1]	C-F Quadr[1]
30%	B-E[1]	C-F Cubic[1]	C-F Quartic[1]	C-F Quadr[2]	C-F Quartic[1]	C-F Cubic[1]	B-E[1]	C-F Quadr[2]
35%	B-E[1]	C-F Cubic[1]	C-F Quadr[2]	C-F Quartic[2]	B-E[1]	C-F Cubic[1]	C-F Quartic[1]	C-F Quadr[2]
40%	B-E[1]	C-F Cubic[1]	C-F Quadr[2]	C-F Quartic[2]	B-E[1]	C-F Cubic[1]	C-F Quartic[1]	C-F Quadr[2]
45%	B-E[1]	C-F Cubic[1]	C-F Quadr[2]	C-F Quartic[3]	B-E[1]	C-F Cubic[1]	C-F Quartic[2]	C-F Quadr[2]
50%	B-E[1]	C-F Cubic[2]	C-F Quadr[2]	C-F Quartic[3]	B-E[1]	C-F Cubic[2]	C-F Quadr[2]	C-F Quartic[2]

TABLE 4

CONTINUED.

	$\eta = 25\%$				$\eta = 30\%$			
CoV	Best	2nd Best	3rd Best	4th Best	Best	2nd Best	3rd Best	4th Best
5%	C-F Cubic[1]	B-E[1]	C-F Quadr[1]	C-F Quartic[1]	C-F Cubic[1]	B-E[1]	C-F Quadr[1]	C-F Quartic[1]
10%	C-F Quadr[1]	C-F Quartic[1]	C-F Cubic[1]	B-E[1]	C-F Cubic[1]	C-F Quadr[1]	B-E[1]	C-F Quartic[1]
15%	C-F Cubic[1]	B-E[1]	C-F Quadr[1]	C-F Quartic[1]	B-E[1]	C-F Cubic[1]	C-F Quadr[1]	C-F Quartic[1]
20%	C-F Cubic[1]	B-E[1]	C-F Quadr[1]	C-F Quartic[1]	C-F Cubic[1]	B-E[1]	C-F Quadr[1]	C-F Quartic[1]
25%	C-F Cubic[1]	B-E[1]	C-F Quartic[1]	C-F Quadr[1]	C-F Cubic[1]	B-E[1]	C-F Quadr[1]	C-F Quartic[1]
30%	C-F Cubic[1]	B-E[1]	C-F Quartic[1]	C-F Quadr[2]	C-F Cubic[1]	B-E[1]	C-F Quadr[1]	C-F Quartic[1]
35%	C-F Cubic[1]	B-E[1]	C-F Quartic[1]	C-F Quadr[2]	C-F Cubic[1]	B-E[1]	C-F Quartic[2]	C-F Quadr[2]
40%	C-F Quartic[1]	B-E[1]	C-F Cubic[1]	C-F Quadr[2]	C-F Cubic[1]	B-E[1]	C-F Quartic[1]	C-F Quadr[2]
45%	B-E[1]	C-F Quartic[1]	C-F Cubic[1]	C-F Quadr[2]	B-E[1]	C-F Cubic[1]	C-F Quartic[1]	C-F Quadr[2]
50%	B-E[1]	C-F Quartic[1]	C-F Cubic[1]	C-F Quadr[2]	B-E[1]	C-F Quartic[1]	C-F Cubic[1]	C-F Quadr[2]

TABLE 5

ANALYSIS OF QUALITY OF APPROXIMATIONS: SUMMARY RESULTS FOR ESTIMATING LOG-NORMAL DISTRIBUTION.

	$\eta = 5\%$				$\eta = 10\%$			
CoV	Best	2nd Best	3rd Best	4th Best	Best	2nd Best	3rd Best	4th Best
5%	C-F Cubic[1]	C-F Quartic[1]	B-E[1]	C-F Quadr[1]	C-F Cubic[1]	B-E[1]	C-F Quartic[1]	C-F Quadr[1]
10%	C-F Cubic[1]	B-E[1]	C-F Quartic[1]	C-F Quadr[1]	C-F Cubic[1]	C-F Quartic[1]	B-E[1]	C-F Quadr[1]
15%	B-E[1]	C-F Cubic[1]	C-F Quadr[1]	C-F Quartic[1]	C-F Quartic[1]	C-F Cubic[1]	B-E[1]	C-F Quadr[1]
20%	B-E[1]	C-F Cubic[1]	C-F Quadr[1]	C-F Quartic[2]	B-E[1]	C-F Cubic[1]	C-F Quartic[1]	C-F Quadr[1]
25%	B-E[1]	C-F Quadr[1]	C-F Cubic[1]	C-F Quartic[2]	B-E[1]	C-F Cubic[1]	C-F Quadr[1]	C-F Quartic[2]
30%	B-E[1]	C-F Quadr[1]	C-F Cubic[1]	C-F Quartic[3]	B-E[1]	C-F Cubic[1]	C-F Quadr[1]	C-F Quartic[2]
35%	C-F Quadr[1]	B-E[1]	C-F Cubic[2]	C-F Quartic[4]	B-E[1]	C-F Quadr[1]	C-F Cubic[2]	C-F Quartic[3]
40%	C-F Quadr[1]	B-E[1]	C-F Cubic[2]	C-F Quartic[4]	B-E[1]	C-F Quadr[1]	C-F Cubic[2]	C-F Quartic[4]
45%	C-F Quadr[1]	B-E[2]	C-F Cubic[3]	C-F Quartic[4]	B-E[1]	C-F Quadr[1]	C-F Cubic[3]	C-F Quartic[4]
50%	C-F Quadr[1]	B-E[2]	C-F Cubic[3]	C-F Quartic[4]	C-F Quadr[1]	B-E[2]	C-F Cubic[3]	C-F Quartic[4]

	$\eta = 15\%$				$\eta = 20\%$			
CoV	Best	2nd Best	3rd Best	4th Best	Best	2nd Best	3rd Best	4th Best
5%	C-F Cubic[1]	C-F Quartic[1]	B-E[1]	C-F Quadr[1]	C-F Cubic[1]	B-E[1]	C-F Quartic[1]	C-F Quadr[1]
10%	C-F Cubic[1]	B-E[1]	C-F Quartic[1]	C-F Quadr[1]	B-E[1]	C-F Cubic[1]	C-F Quadr[1]	C-F Quartic[1]
15%	C-F Cubic[1]	B-E[1]	C-F Quartic[1]	C-F Quadr[1]	C-F Cubic[1]	B-E[1]	C-F Quartic[1]	C-F Quadr[1]
20%	C-F Quartic[1]	C-F Cubic[1]	B-E[1]	C-F Quadr[1]	C-F Cubic[1]	B-E[1]	C-F Quartic[1]	C-F Quadr[1]
25%	B-E[1]	C-F Cubic[1]	C-F Quartic[1]	C-F Quadr[1]	C-F Cubic[1]	B-E[1]	C-F Quartic[1]	C-F Quadr[1]
30%	B-E[1]	C-F Cubic[1]	C-F Quartic[2]	C-F Quadr[2]	C-F Quartic[1]	B-E[1]	C-F Cubic[1]	C-F Quadr[2]
35%	B-E[1]	C-F Cubic[2]	C-F Quadr[2]	C-F Quartic[2]	B-E[1]	C-F Quartic[1]	C-F Cubic[1]	C-F Quadr[2]
40%	B-E[1]	C-F Quadr[2]	C-F Cubic[2]	C-F Quartic[3]	B-E[1]	C-F Cubic[2]	C-F Quartic[2]	C-F Quadr[2]
45%	B-E[1]	C-F Quadr[2]	C-F Cubic[3]	C-F Quartic[3]	B-E[1]	C-F Quadr[2]	C-F Cubic[2]	C-F Quartic[3]
50%	B-E[1]	C-F Quadr[2]	C-F Cubic[3]	C-F Quartic[4]	B-E[1]	C-F Quadr[2]	C-F Cubic[3]	C-F Quartic[3]

TABLE 5

CONTINUED.

	$\eta = 25\%$				$\eta = 30\%$			
CoV	Best	2nd Best	3rd Best	4th Best	Best	2nd Best	3rd Best	4th Best
5%	C-F Cubic[1]	B-E[1]	C-F Quadr[1]	C-F Quartic[1]	C-F Cubic[1]	B-E[1]	C-F Quadr[1]	C-F Quartic[1]
10%	C-F Quadr[1]	C-F Quartic[1]	C-F Cubic[1]	B-E[1]	C-F Cubic[1]	C-F Quadr[1]	B-E[1]	C-F Quartic[1]
15%	C-F Cubic[1]	B-E[1]	C-F Quadr[1]	C-F Quartic[1]	B-E[1]	C-F Cubic[1]	C-F Quadr[1]	C-F Quartic[1]
20%	C-F Cubic[1]	B-E[1]	C-F Quadr[1]	C-F Quartic[1]	C-F Cubic[1]	B-E[1]	C-F Quadr[1]	C-F Quartic[1]
25%	C-F Cubic[1]	B-E[1]	C-F Quartic[1]	C-F Quadr[1]	C-F Cubic[1]	B-E[1]	C-F Quadr[1]	C-F Quartic[1]
30%	C-F Cubic[1]	B-E[1]	C-F Quartic[1]	C-F Quadr[2]	C-F Cubic[1]	B-E[1]	C-F Quadr[2]	C-F Quartic[2]
35%	B-E[1]	C-F Quartic[1]	C-F Cubic[1]	C-F Quadr[2]	C-F Cubic[1]	B-E[1]	C-F Quartic[2]	C-F Quadr[2]
40%	C-F Quartic[1]	B-E[1]	C-F Cubic[2]	C-F Quadr[2]	B-E[1]	C-F Cubic[1]	C-F Quartic[2]	C-F Quadr[2]
45%	B-E[1]	C-F Quartic[1]	C-F Cubic[2]	C-F Quadr[2]	B-E[1]	C-F Quartic[1]	C-F Cubic[2]	C-F Quadr[2]
50%	B-E[1]	C-F Quartic[2]	C-F Quadr[2]	C-F Cubic[3]	B-E[1]	C-F Quartic[1]	C-F Cubic[2]	C-F Quadr[3]

TABLE 6

ANALYSIS OF QUALITY OF APPROXIMATIONS: SUMMARY RESULTS FOR ESTIMATING INVERSE-GAMMA DISTRIBUTION.

	$\eta = 5\%$				$\eta = 10\%$			
CoV	Best	2nd Best	3rd Best	4th Best	Best	2nd Best	3rd Best	4th Best
5%	C-F Cubic[1]	C-F Quartic[1]	B-E[1]	C-F Quadr[1]	B-E[1]	C-F Cubic[1]	C-F Quadr[1]	C-F Quartic[1]
10%	C-F Cubic[1]	B-E[1]	C-F Quartic[1]	C-F Quadr[1]	C-F Cubic[1]	B-E[1]	C-F Quartic[1]	C-F Quadr[1]
15%	B-E[1]	C-F Cubic[1]	C-F Quadr[1]	C-F Quartic[2]	C-F Quartic[1]	C-F Cubic[1]	B-E[1]	C-F Quadr[1]
20%	B-E[1]	C-F Quadr[1]	C-F Cubic[1]	C-F Quartic[3]	B-E[1]	C-F Cubic[1]	C-F Quadr[1]	C-F Quartic[2]
25%	C-F Quadr[1]	B-E[1]	C-F Cubic[2]	C-F Quartic[4]	B-E[1]	C-F Quadr[2]	C-F Cubic[2]	C-F Quartic[3]
30%	C-F Quadr[1]	B-E[2]	C-F Cubic[3]	C-F Quartic[4]	B-E[1]	C-F Quadr[2]	C-F Cubic[3]	C-F Quartic[3]
35%	C-F Quadr[1]	B-E[2]	C-F Cubic[4]	C-F Quartic[4]	C-F Quadr[1]	B-E[2]	C-F Cubic[4]	C-F Quartic[4]
40%	C-F Quadr[1]	B-E[3]	C-F Cubic[4]	C-F Quartic[4]	C-F Quadr[1]	B-E[2]	C-F Quartic[4]	C-F Cubic[4]
45%	C-F Quadr[2]	B-E[3]	C-F Quartic[4]	C-F Cubic[4]	C-F Quadr[1]	B-E[3]	C-F Quartic[4]	C-F Cubic[4]
50%	C-F Quadr[3]	B-E[4]	C-F Quartic[4]	C-F Cubic[4]	C-F Quadr[1]	B-E[4]	C-F Quartic[4]	C-F Cubic[4]
	$\eta = 15\%$				$\eta = 20\%$			
CoV	Best	2nd Best	3rd Best	4th Best	Best	2nd Best	3rd Best	4th Best
5%	C-F Cubic[1]	C-F Quartic[1]	B-E[1]	C-F Quadr[1]	C-F Cubic[1]	B-E[1]	C-F Quadr[1]	C-F Quartic[1]
10%	C-F Cubic[1]	B-E[1]	C-F Quadr[1]	C-F Quartic[1]	B-E[1]	C-F Cubic[1]	C-F Quadr[1]	C-F Quartic[1]
15%	C-F Cubic[1]	B-E[1]	C-F Quartic[1]	C-F Quadr[1]	C-F Cubic[1]	B-E[1]	C-F Quadr[1]	C-F Quartic[1]
20%	C-F Quartic[1]	C-F Cubic[1]	B-E[1]	C-F Quadr[2]	C-F Cubic[1]	B-E[1]	C-F Quartic[1]	C-F Quadr[2]
25%	B-E[1]	C-F Quartic[1]	C-F Cubic[2]	C-F Quadr[2]	B-E[1]	C-F Cubic[1]	C-F Quartic[1]	C-F Quadr[2]
30%	B-E[1]	C-F Quadr[2]	C-F Quartic[2]	C-F Cubic[2]	C-F Quartic[1]	B-E[1]	C-F Cubic[2]	C-F Quadr[2]
35%	B-E[1]	C-F Quadr[2]	C-F Quartic[3]	C-F Cubic[3]	B-E[1]	C-F Quartic[1]	C-F Quadr[2]	C-F Cubic[3]
40%	B-E[2]	C-F Quadr[2]	C-F Quartic[3]	C-F Cubic[4]	B-E[1]	C-F Quartic[2]	C-F Quadr[2]	C-F Cubic[4]
45%	C-F Quadr[2]	B-E[3]	C-F Quartic[4]	C-F Cubic[4]	B-E[2]	C-F Quadr[2]	C-F Quartic[2]	C-F Cubic[4]
50%	C-F Quadr[1]	B-E[3]	C-F Quartic[4]	C-F Cubic[4]	C-F Quadr[2]	C-F Quartic[3]	B-E[3]	C-F Cubic[4]

TABLE 6

CONTINUED.

	$\eta = 25\%$				$\eta = 30\%$			
CoV	Best	2nd Best	3rd Best	4th Best	Best	2nd Best	3rd Best	4th Best
5%	C-F Cubic[1]	B-E[1]	C-F Quadr[1]	C-F Quartic[1]	C-F Cubic[1]	B-E[1]	C-F Quadr[1]	C-F Quartic[1]
10%	C-F Quadr[1]	C-F Cubic[1]	B-E[1]	C-F Quartic[1]	C-F Cubic[1]	C-F Quadr[1]	B-E[1]	C-F Quartic[1]
15%	C-F Cubic[1]	B-E[1]	C-F Quadr[1]	C-F Quartic[1]	B-E[1]	C-F Cubic[1]	C-F Quadr[1]	C-F Quartic[1]
20%	C-F Cubic[1]	B-E[1]	C-F Quadr[1]	C-F Quartic[2]	C-F Cubic[1]	B-E[1]	C-F Quadr[1]	C-F Quartic[2]
25%	C-F Cubic[1]	B-E[1]	C-F Quadr[2]	C-F Quartic[2]	C-F Cubic[1]	B-E[1]	C-F Quadr[2]	C-F Quartic[2]
30%	B-E[1]	C-F Cubic[2]	C-F Quartic[2]	C-F Quadr[2]	B-E[1]	C-F Cubic[1]	C-F Quadr[2]	C-F Quartic[3]
35%	B-E[1]	C-F Quartic[2]	C-F Quadr[3]	C-F Cubic[3]	B-E[1]	C-F Cubic[2]	C-F Quadr[3]	C-F Quartic[3]
40%	B-E[1]	C-F Quartic[2]	C-F Quadr[3]	C-F Cubic[4]	B-E[1]	C-F Quadr[3]	C-F Quartic[3]	C-F Cubic[3]
45%	C-F Quartic[1]	B-E[2]	C-F Quadr[3]	C-F Cubic[4]	B-E[1]	C-F Quartic[3]	C-F Quadr[3]	C-F Cubic[4]
50%	C-F Quartic[1]	B-E[2]	C-F Quadr[3]	C-F Cubic[4]	B-E[2]	C-F Quartic[3]	C-F Quadr[3]	C-F Cubic[4]

TABLE 7

THE CASES WHERE THE B-E APPROXIMATION IS OUTPERFORMED BY THE C-F APPROXIMATIONS.

Case #	Distribution	η	CoV	Rank of Approx	Quality Band of B-E Approx	Best Approx & Quality Band
1	Log-Normal	5%	45%	2nd Best	2	C-F Quadratic [1]
2	Log-Normal	5%	50%	2nd Best	2	C-F Quadratic [1]
3	Log-Normal	10%	50%	2nd Best	2	C-F Quadratic [1]
4	Inverse-Gamma	5%	30%	2nd Best	2	C-F Quadratic [1]
5	Inverse-Gamma	5%	35%	2nd Best	2	C-F Quadratic [1]
6	Inverse-Gamma	5%	40%	2nd Best	3	C-F Quadratic [1]
7	Inverse-Gamma	5%	45%	2nd Best	3	C-F Quadratic [2]
8	Inverse-Gamma	5%	50%	2nd Best	4	C-F Quadratic [3]
9	Inverse-Gamma	10%	35%	2nd Best	2	C-F Quadratic [1]
10	Inverse-Gamma	10%	40%	2nd Best	2	C-F Quadratic [1]
11	Inverse-Gamma	10%	45%	2nd Best	3	C-F Quadratic [1]
12	Inverse-Gamma	10%	50%	2nd Best	4	C-F Quadratic [1]
13	Inverse-Gamma	15%	45%	2nd Best	3	C-F Quadratic [2]
14	Inverse-Gamma	15%	50%	2nd Best	3	C-F Quadratic [1]
15	Inverse-Gamma	20%	50%	3rd Best	3	C-F Quadratic [2]
16	Inverse-Gamma	25%	45%	2nd Best	2	C-F Quartic [1]
17	Inverse-Gamma	25%	50%	2nd Best	2	C-F Quartic [1]

falling into band 1, can be outperformed by either (1) C-F Quadratic (first-order Normal Power) approximation; or (2) C-F Quartic approximation.

These 17 cases are summarised and provided in Table 7.

As can be seen from Table 7 above, the B-E approximation fails to be "the best" only in extreme situations of reserve risk profile with high volatility (i.e. CoV) and/or excessive relative skewness (i.e. SC ratio). In most cases (15 out of 17), it is outperformed by the C-F Quadratic (or equivalently Normal Power) approximation, and only in two cases, when used for highly volatile (CoV $\geqslant$ 45%) and excessively skewed (SC $\geqslant$ 5) Inverse-Gamma reserve distribution along with the relative risk margin of 25%, it is outperformed by the C-F Quartic approximation. Out of those two cases, it really comes down to one case — the case 17 of the Inverse-Gamma distribution with CoV = 50%, for which the absolute value of relative delta error of the B-E approximation is about 2.2%, as for the case 16 the relative delta error is just above 1%, giving the B-E approximation the adherence quality close to that of band 1 (see the detailed outputs of the analysis of quality of PoS approximations corresponding to cases 16 and 17 in Appendix C).

It should also be noted that there are two cases where the B-E approximation, whilst being "the best approximation", falls into band 2 of adherence quality. Again, those are rather extreme cases of the Inverse-Gamma distribution with relatively high volatility (CoV $\geqslant$ 45%) and excessive skewness (SC $\geqslant$ 5).

4. PoS APPROXIMATIONS — PORTFOLIO OF MULTIPLE RESERVING CLASSES

This section focuses on providing approximation formulae for PoS of diversified risk margin of the portfolio of multiple reserving classes. As indicated in Section 2, we assume that the centralised and normalised copy of reserve value X_i of the ith class, $\widetilde{X}_i$, is estimated by the Fleishman polynomial structure of a standard normal random variable. In particular, we consider the following two different cases:

- $X_i \sim P_2(Z_i) = a_i Z_i + b_i \left(Z_i^2 - 1\right)$ — suitable for estimating skewness of the reserving portfolio risk profile when the risk margin is approximated using skewness only;
- $X_i \sim P_3(Z_i) = a_i Z_i + b_i \left(Z_i^2 - 1\right) + c_i Z_i^3$ — suitable for estimating skewness and kurtosis of the reserving portfolio risk profile when the risk margin is approximated using both skewness and kurtosis.

The coefficients of polynomials P_2 and P_3 are calibrated using the method of moments by matching the second and third moments of $P_2(Z_i)$ and the second, third and fourth moments of $P_3(Z_i)$ to 1 (standard deviation of $\widetilde{X}_i$), γ_i (skewness of X_i) and $\iota_i + 3$ (non-centralised or absolute kurtosis[18] of X_i), respectively.

The coefficients of P_2 can be analytically expressed by solving the following system of equations:

$$\begin{cases} 1 = a_i^2 + 2b_i^2, \\ \gamma_i = 6a_i^2 b_i + 8b_i^3 \end{cases} . \tag{38}$$

The system (38) is reduced to

$$\begin{cases} a_i = \sqrt{1 - 2b_i^2}, \\ \gamma_i = 6b_i - 4b_i^3 \end{cases} \tag{39}$$

from where we get

$$\begin{cases} a_i = \sqrt{1 - 2b_i^2}, \\ b_i = \text{a real root of cubic equation in (39).} \end{cases} \tag{40}$$

From (39) it follows that $|b_i| \leqslant \frac{1}{\sqrt{2}}$ and thus $0 \leqslant \gamma_i \leqslant 2\sqrt{2}$, which may indicate that it is not suitable for the types of reserve risk profile that are adhering to Inverse-Gamma parametric distribution and have CoV above 50%. The discriminant D of cubic equation in (39) is equal to $\frac{\gamma_i^2}{64} - \frac{1}{8}$ and is negative for $\gamma_i < 2\sqrt{2}$, indicating that there are three real roots as defined in (28): "root 1" x_1, "root 2" x_2 and "root 3" x_3. By analysing those roots as functions of γ_i, we could eliminate the roots, which fall outside the interval of admissible values of b_i, $(-\frac{1}{\sqrt{2}}, \frac{1}{\sqrt{2}})$. Figure 4 shows that there is only one suitable root for b_i and that is "root 3", which equals $\sqrt{2}\cos(\frac{\varphi}{3} + \frac{4\pi}{3})$.

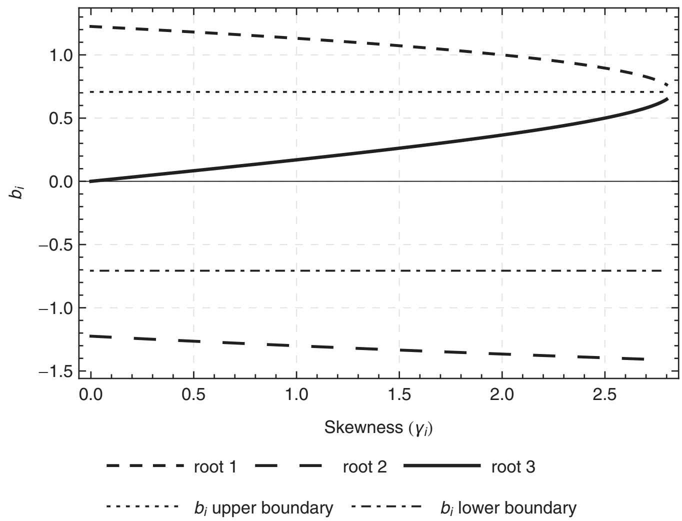

FIGURE 4: Real roots of cubic equation in (39).

The coefficients of P_3 are calibrated numerically. Their values are pre-computed and tabulated in Appendix A for different levels of CoV and the four parametric distributions (DoAs) from $\mathcal{PD}$.

4.1. Estimation of skewness and kurtosis of reserving portfolio

We define the total reserve value across the portfolio of m reserving classes as

$$X_\Sigma = \sum_{i=1}^{m} X_i, \tag{41}$$

where each ith class reserve value is approximated by Fleishman polynomial of a standard normal random variable

$$X_i \approx \mathrm{BE}_i \cdot (1 + \mathrm{CoV}_i \cdot P_3(Z_i)). \tag{42}$$

It is clear that $\mathrm{BE}_\Sigma = \sum_{i=1}^{m} \mathrm{BE}_i$. It should be noted that setting $c_i = 0$ reduces the problem to simply approximating $X_i \approx \mathrm{BE}_i \cdot (1 + \mathrm{CoV}_i \cdot P_2(Z_i))$.

As set up in Assumption 3 in Section 2 all the standlone reserve risk profiles interacts between each other according to a Gaussian dependence structure and that the linear correlations ρ_{ij} (coefficients of a Gaussian copula) are derived from the pre-calibrated rank correlation assumptions.

The aim of this subsection is to compute the second, third and fourth central moments of the reserving portfolio distribution and derive their corresponding coefficient of variation CoV_Σ, skewness γ_Σ and kurtosis ι_Σ. Then those values would be further used to compute SC and KCsq ratios to determine the domain of attraction to one of the four parametric distributions from $\mathcal{PD}$ and then estimate the PoS of the diversified risk margin η_Σ at the portfolio level by using the approximation formulae already derived in Section 3.

Coefficient of Variation. We compute the variance of X_Σ:

$$\begin{aligned}
\mathrm{Var}[X_\Sigma] &= \mathbb{E}\left[\left(\sum_{i=1}^{m}\sigma_i \cdot P_3(Z_i)\right)^2\right] \\
&= \sum_{i=1}^{m}\sigma_i^2 \cdot \mathbb{E}\left[P_3^2(Z_i)\right] + 2\sum_{ij}\sigma_i\sigma_j \cdot \mathbb{E}\left[P_3(Z_i)P_3(Z_j)\right] \\
&= \sum_{i=1}^{m}\sigma_i^2 + 2\sum_{ij}\sigma_i\sigma_j \cdot \mathbb{E}\left[P_3(Z_i)P_3(Z_j)\right], \qquad (43)
\end{aligned}$$

where $\sigma_i = \mathrm{BE}_i \cdot \mathrm{CoV}_i$, and $\mathbb{E}\left[P_3^2(Z_i)\right] = 1$ as the Fleishman polynomial coefficients are calibrated so that the polynomial has unit variance. The following components of the formula (43) above are derived in Appendix B and provided here

$$\begin{aligned}
\mathbb{E}\left[P_3(Z_i)P_3(Z_j)\right] = \rho_{ij}\big(&a_ia_j + 2b_ib_j\rho_{ij} + 3\left(a_ic_j + a_jc_i\right) \\
&+3c_ic_j\left(3 + 2\rho_{ij}^2\right)\big). \qquad (44)
\end{aligned}$$

When P_2 polynomial is used, i.e. $c_i = 0$, then this component is reduced to

$$\mathbb{E}\left[P_3(Z_i)P_3(Z_j)\right] = \rho_{ij}\left(a_ia_j + 2b_ib_j\rho_{ij}\right). \qquad (45)$$

Then, CoV_Σ^2 is equal to

$$\begin{aligned}
\mathrm{CoV}_\Sigma^2 &= \frac{\mathrm{Var}[X_\Sigma]}{\mathrm{BE}_\Sigma^2} \\
&= \sum_{i=1}^{m} w_i^2\,\mathrm{CoV}_i^2 + 2\sum_{ij} w_i\,w_j\,\mathrm{CoV}_i\,\mathrm{CoV}_j \cdot \mathbb{E}\left[P_3(Z_i)P_3(Z_j)\right], \qquad (46)
\end{aligned}$$

where $w_i = \frac{\mathrm{BE}_i}{\mathrm{BE}_\Sigma}$.

https://doi.org/10.1017/asb.2017.12 Published online by Cambridge University Press

Skewness. We compute the third central moment of X_Σ:

$$\begin{aligned}\mathbb{E}\left[(X_\Sigma - \mathrm{BE}_\Sigma)^3\right] &= \mathbb{E}\left[\left(\sum_{i=1}^{m}\sigma_i \cdot P_3(Z_i)\right)^3\right] \\ &= \sum_{i=1}^{m}\sigma_i^3 \cdot \gamma_i + 3\sum_{ij}\sigma_i^2\sigma_j \cdot \mathbb{E}\left[P_3(Z_i)^2 P_3(Z_j)\right] \\ &\quad + 6\sum_{ijk}\sigma_i\sigma_j\sigma_k \cdot \mathbb{E}\left[P_3(Z_i)P_3(Z_j)P_3(Z_k)\right], \end{aligned} \tag{47}$$

where $\mathbb{E}[P_3^3(Z_i)] = \gamma_i$, as the Fleishman polynomial coefficients are calibrated so that the polynomial has skewness γ_i for ith standalone risk profile. In formula (47), the summation term with multiple 3 has $\binom{m}{2}$ different sub-terms, and the summation term with multiple 6 is relevant if $m \geqslant 3$ and has $\binom{m}{3}$ different sub-terms.

The following components of the formula (47) are derived in Appendix B and provided here only for the partial case when P_2 is used, i.e. $c_i = 0$:

$$\mathbb{E}\left[P_3(Z_i)^2 P_3(Z_j)\right] = 2\rho_{ij}\left(2a_i a_j b_i + \left(a_i^2 + 4b_i^2\right) b_j \rho_{ij}\right) \tag{48}$$

$$\begin{aligned}\mathbb{E}\left[P_3(Z_i)P_3(Z_j)P_3(Z_k)\right] &= 2\left(a_j a_k b_i \rho_{ij}\rho_{ik} + a_j a_i b_k \rho_{jk}\rho_{ik}\right. \\ &\quad \left. + a_i a_k b_j \rho_{ij}\rho_{ik}\right) + 8 b_i b_j b_k \rho_{ij}\rho_{ik}\rho_{jk}. \end{aligned} \tag{49}$$

The skewness γ_Σ is then calculated as follows

$$\gamma_\Sigma = \frac{\mathbb{E}\left[(X_\Sigma - \mathrm{BE}_\Sigma)^3\right]}{(\mathrm{BE}_\Sigma\,\mathrm{CoV}_\Sigma)^3}. \tag{50}$$

Kurtosis. To compute the fourth central moment of X_Σ, we use the Multinomial formula and apply the expectation operator:

$$\begin{aligned}\mathbb{E}\left[(X_\Sigma - \mathrm{BE}_\Sigma)^4\right] &= \mathbb{E}\left[\left(\sum_{i=1}^{m}\sigma_i \cdot P_3(Z_i)\right)^4\right] \\ &= \sum_{n_1+n_2+\cdots+n_m=4}\binom{4}{n_1,\, n_2, \ldots,\, n_m}\mathbb{E}\left[\prod_{k=1}^{m}\sigma_k^{n_k} \cdot P(Z_k)^{n_k}\right]\end{aligned}$$

https://doi.org/10.1017/asb.2017.12 Published online by Cambridge University Press

$$
\begin{aligned}
&= \sum_{i=1}^{m} \sigma_i^4 \cdot (\iota_i + 3) + 4 \sum_{ij} \sigma_i^3 \sigma_j \cdot \mathbb{E}\left[P_3(Z_i)^3 P_3(Z_j)\right] \\
&\quad + 6 \sum_{ij} \sigma_i^2 \sigma_j^2 \cdot \mathbb{E}\left[P_3(Z_i)^2 P_3(Z_j)^2\right] \\
&\quad + 12 \sum_{ijk} \sigma_i^2 \sigma_j \sigma_k \cdot \mathbb{E}\left[P_3(Z_i)^2 P_3(Z_j) P_3(Z_k)\right] \\
&\quad + 24 \sum_{ijkl} \sigma_i \sigma_j \sigma_k \sigma_l \cdot \mathbb{E}\left[P_3(Z_i) P_3(Z_j) P_3(Z_k) P_3(Z_l)\right] \qquad (51)
\end{aligned}
$$

where $\mathbb{E}\left[P_3^4(Z_i)\right] = \iota_i + 3$, as the Fleishman polynomial coefficients are calibrated so that the polynomial has absolute[19] kurtosis value of $\iota_i + 3$ for ith standalone risk profile. The components of the portfolio skewness formula (51) are derived in Appendix B. Their formulaic expressions are too long to be presented here.

The kurtosis ι_Σ is then calculated as follows:

$$
\iota_\Sigma = \frac{\mathbb{E}\left[(X_\Sigma - \mathrm{BE}_\Sigma)^4\right]}{(\mathrm{BE}_\Sigma \, \mathrm{CoV}_\Sigma)^4} - 3. \qquad (52)
$$

5. Practical implementations and numerical illustrations

This section discusses some ideas of practical implementation of the PoS approximations and provides numerical illustrations.

5.1. Notes on practical implementations

PoS approximation — standalone risk margin. From the analysis of quality of the four proposed PoS approximations performed in Section 3.4, it is evident that there are two that stand out — (1) B-E approximation; and (2) C-F Quadratic (or equivalently Normal Power) approximation. Both are generally of highest quality and very simple to use when compared to the other two: C-F Cubic and C-F Quartic approximations. In particular, the B-E approximation in most cases is either ranked as “the best approximation” or, if not “the best”, then still falling into the highest quality band and at the same time being superior to others due to its extreme simplicity. There were a few situations where the B-E approximation is neither being “the best” nor falling into the highest quality band and the C-F Quadratic approximation would serve as “the best approximation”. It should also be noted that very occasionally the B-E approximation can be outperformed by the C-F Quartic approximation. However, the loss in its adherence quality is insignificant and its relative error of approximation

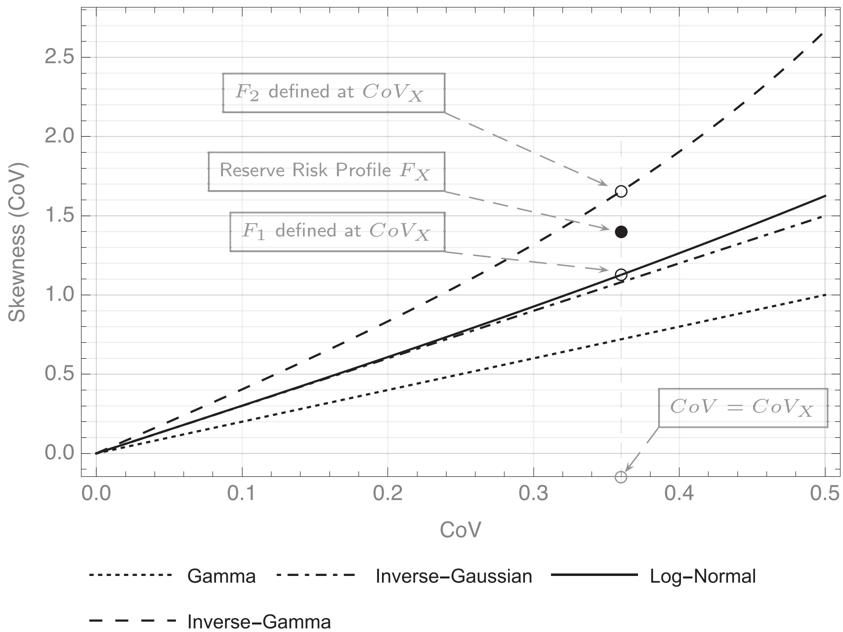

FIGURE 5: Locating reserve risk profile — illustration.

does not exceed 2.2%, making it still possible to use the B-E approximation by ultimately fine tuning it (see the implementation algorithm below) using fairly reasonable error reducing correction factors.

So, when it comes to practical implementation, the choice of the most suitable PoS approximation would then ideally be limited to those two approximations — B-E and C-F Quadratic.

Given the above, one could easily implement the estimation of PoS level in Excel using the following algorithmic steps:

1. For a given reserve X for which its risk profile F_X is characterised by its best estimate BE_X, coefficient of variation CoV_X and skewness γ_X, compute SC_X to identify the relative location of the reserve risk profile F_X with respect to the four parametric distributions from $\mathcal{PD}$. Let F_X be located between two known parametric distributions F_1 and F_2 from $\mathcal{PD}$ (see Figure 5). Here, the location would be determined by computing the SC ratio for the parametric distributions from $\mathcal{PD}$ given the $\text{CoV}(= \text{CoV}_X)$ level and comparing them against SC_X.
2. For given reserve volatility level CoV_X and risk margin η_X identify the best PoS approximation out of the two — B-E and C-F Quadratic, by taking the following steps:

- for each adjacent parametric distribution F_i, $i = 1, 2$, calculate both
  - exact PoS value, PoS_i, using the value of $F_i(1 + \eta_X)$ defined in Section 3.4 (see the formulae for exact PoS value of each of the four parametric distributions from $\mathcal{PD}$); and also
  - its estimate, $\widehat{\text{PoS}}_{A,i}$, based on the PoS approximation A from {B-E, C-F Qudratic}, using formulae (14), (17) and (18), and also assuming $\gamma_i = \text{SC}_i(\text{CoV}_X) \cdot \text{CoV}_X$ with SC_i being defined in Table 1 on page 744;
- use the above values to compute the relative error of approximation $\Delta_{A,i} = \frac{\text{PoS}_i - \widehat{\text{PoS}}_{A,i}}{\widehat{\text{PoS}}_{A,i}}$;
- the best PoS approximation A^* is then such that has the smallest sum of absolute values of relative error on the two adjacent curves, i.e.

$$A^* = \arg \min_{A \in \{\text{B-E, C-F Qudratic}\}} \left|\Delta_{A,1}\right| + \left|\Delta_{A,2}\right|.$$

3. For A^* and the two adjacent parametric distributions F_1 and F_2 from $\mathcal{PD}$, calculate corresponding correction factors $g_i = 1 + \Delta_{A^*,i}$ at (CoV_X, η_X), and then find the correction factor g_X for reserve risk profile F_X by interpolating between the two factors g_i, $i = 1, 2$. Here, the interpolation is done in relation to linear proximity of $\text{SC}_X(\text{CoV}_X)$ ratio to analogous ratios of F_1 and F_2 curves at CoV_X, i.e.

$$g_X = g_1 + \frac{\text{SC}_X - \text{SC}_1}{\text{SC}_2 - \text{SC}_1} \cdot (g_2 - g_1).$$

4. Given the chosen PoS approximation A^*, compute the estimated PoS level, $\widehat{\text{PoS}}_{A^*,X}$ of risk margin η_X of reserve risk profile F_X with volatility CoV_X and relative skewness SC_X, and then adjust it by multiplying it by the correction factor g_X obtained in the preceding step to get the final estimate $\widetilde{\text{PoS}}_{A^*,X}$.

It is quite possible to have a situation where a particular reserve risk profile is in the DoA induced by Inverse-Gamma, but yet relatively more skewed than Inverse-Gamma. In that case, the above algorithm would not quite work, as the reserve risk profile would be outside the range of the four parametric distributions from $\mathcal{PD}$, and one would need to use extrapolation to find the corresponding correction factor. To avoid extrapolation and make the above algorithm work, one may introduce another parametric distribution of $\mathcal{SSP}$ type that is relatively more skewed than the given reserve risk profile, thus allowing to locate the reserve risk profile between itself and Inverse-Gamma distribution. One of the examples of such $\mathcal{SSP}$ distribution is *Log-Logistic (Fisk)*

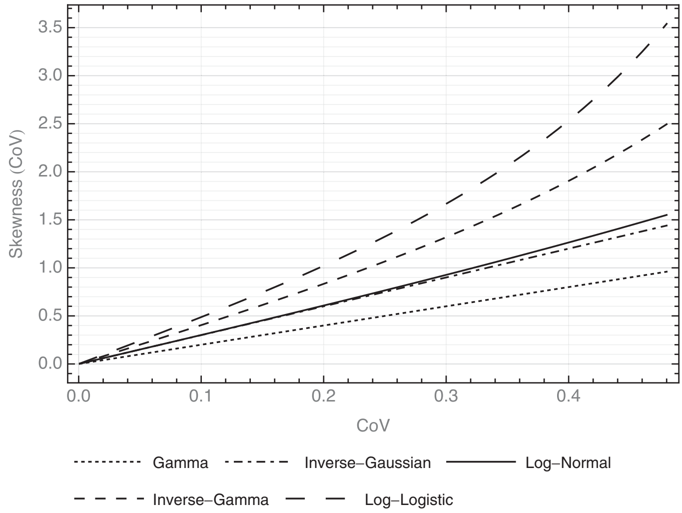

FIGURE 6: Log-Logistic distribution in the CoV-Skewness system of coordinates.

distribution with the following characteristics:

$$\begin{aligned}
\text{CDF:}\quad & \mathrm{CDF}_{LL}(x) = F_{\beta,\alpha}(x) = \frac{1}{1+\left(\frac{x}{\alpha}\right)^{-\beta}}, \; x > 0,\; \alpha > 0,\; \beta > 0;\\
\text{Mean:}\quad & M_{LL} = \frac{\beta\pi}{\alpha}\,\csc\left(\frac{\pi}{\alpha}\right),\; \alpha > 1;\\
\text{CoV:}\quad & \mathrm{CoV}_{LL} = \sin\left(\frac{\pi}{\alpha}\right)\sqrt{\frac{2\alpha\,\csc\left(\frac{2\pi}{\alpha}\right)}{\pi} - \csc^2\left(\frac{\pi}{\alpha}\right)},\; \alpha > 2;\\
\text{SC ratio:}\quad & \mathrm{SC}_{LL} = \frac{\csc\left(\frac{\pi}{\alpha}\right)\left[2\pi^2\csc^3\left(\frac{\pi}{\alpha}\right) - 6\alpha\pi\csc\left(\frac{\pi}{\alpha}\right)\csc\left(\frac{2\pi}{\alpha}\right) + 3\alpha^2\csc\left(\frac{3\pi}{\alpha}\right)\right]}{\left[\pi\csc^2\left(\frac{\pi}{\alpha}\right) - 2\alpha\csc\left(\frac{2\pi}{\alpha}\right)\right]^2},\; \alpha > 3.
\end{aligned} \tag{53}$$

The location of Log-Logistic distribution in the CoV-Skewness system of coordinates with respect to the four parametric distributions from $\mathcal{PD}$ is illustrated in Figure 6.

To compute the exact value of PoS for a reserve risk profile with Log-Logistic distribution, one would need to get the reserve risk profile CDF normalised by its mean evaluated at $1 + \eta_X$, i.e. compute $F_{\beta'(\widehat{\alpha}),\widehat{\alpha}}(1 + \eta_X)$, where

$$\widehat{\alpha} = \underset{\alpha > 3}{\arg\text{solve}}\ \{\mathrm{CoV}_{LL}(\alpha) = \mathrm{CoV}_X\}; \tag{54}$$

$$\beta' = \frac{\widehat{\alpha}}{\pi}\sin\left(\frac{\pi}{\widehat{\alpha}}\right). \tag{55}$$

The parameter $\widehat{\alpha}$ in (54) can be easily found using Excel solver.

To compute the PoS estimate using the approximation $A \in \{\text{B-E, C-F Qudratic}\}$, one would need to use volatility CoV_{LL} set at CoV_X and skewness $\gamma_{LL} = \mathrm{SC}_{LL}(\widehat{\alpha}) \cdot \mathrm{CoV}_{LL}$.

PoS approximation — risk margin of reserve portfolio. The implementation of PoS approximation of diversified risk margin η_Σ of a portfolio consisting of m

reserving classes is rather straightforward and can be easily done in Excel. The idea is to compute volatility CoV_Σ and skewness γ_Σ at the portfolio level using the known characteristics (best estimate, coefficient of variance and skewness) of each reserving class. Then, the obtained values CoV_Σ and γ_Σ are used to get the PoS estimate of η_Σ using the algorithm defined on page 774 in the preceding subsection.

To compute CoV_Σ and γ_Σ, one would need to use formulae (46)–(45) and (47)–(50), respectively. In there, the Fleishman coefficients $a_{\cdot\cdot}$ and $b_{\cdot\cdot}$ are calculated using formula (40), with $b_{\cdot\cdot}$ being the third root of cubic equation defined in (39). The correlation coefficients $\rho_{\cdot\cdot}$ are computed from the given rank correlations $r_{\cdot\cdot}$ between reserving classes using formula (5).

5.2. Numerical illustrations

PoS approximation — standalone risk margin. Consider the reserve X for which its risk profile F_X is characterised by its volatility $\mathrm{CoV}_X = 36\%$ and skewness $\gamma_X = 1.4$. It is assumed that its technical provision is booked using the risk margin $\eta = 11\%$. The following demonstrates how the PoS estimate can be derived using the algorithm defined on page 774 in Section 5.1.

1. The implied $\mathrm{SC}_X = \frac{\gamma_X}{\mathrm{CoV}_X} = 3.8889$ and therefore the risk profile F_X is located between the two known parametric distributions: Log-Normal (F_1) and Inverse-Gamma (F_2), as

$$\mathrm{SC}_{\mathrm{LN}} = 3 + 0.36^2 = 3.1296 < \mathrm{SC}_X = 3.8889 < \mathrm{SC}_{\mathrm{IGa}} = \frac{4}{1 - 0.36^2} = 4.5956;$$

2. For given reserve volatility level CoV_X and risk margin η_X, we follow the step 2 of the algorithm defined on page 774 in Section 5.1 to identify the best PoS approximation out of the two — B-E and C-F Quadratic. The following table summarises the calculation results and helps us conclude

Approxim Type	PoS Reserve Risk Profile	PoS LN	PoS IGa	PoS (exact) LN	PoS (Exact) IGa	g_{LN}	g_{IGa}	Δ_{LN}	Δ_{IGa}
B-E	69.773%	68.300%	71.118%	68.207%	70.268%	0.998631	0.988037	−0.137%	−1.196%
C-F Quadr	68.587%	67.528%	69.486%	68.207%	70.268%	1.010057	1.011252	1.006%	1.125%

that B-E approximation is the best as $|-0.137\%| + |-1.196\%| = 1.333\% < 2.131\% = |1.006\%| + |1.125\%|$.

3. Knowing that the best PoS approximation A^* is B-E, we proceed to find the correction factor for our reserve risk profile by interpolating the corresponding correction factors for Log-Normal and Inverse-Gamma curves obtained in the table above from the previous step:

$$g_X = g_{LN} + \frac{\mathrm{SC}_X - \mathrm{SC}_{LN}}{\mathrm{SC}_{IGa} - \mathrm{SC}_{LN}} \cdot (g_{\mathrm{IGa}} - g_{\mathrm{LN}}) = 0.993144.$$

https://doi.org/10.1017/asb.2017.12 Published online by Cambridge University Press

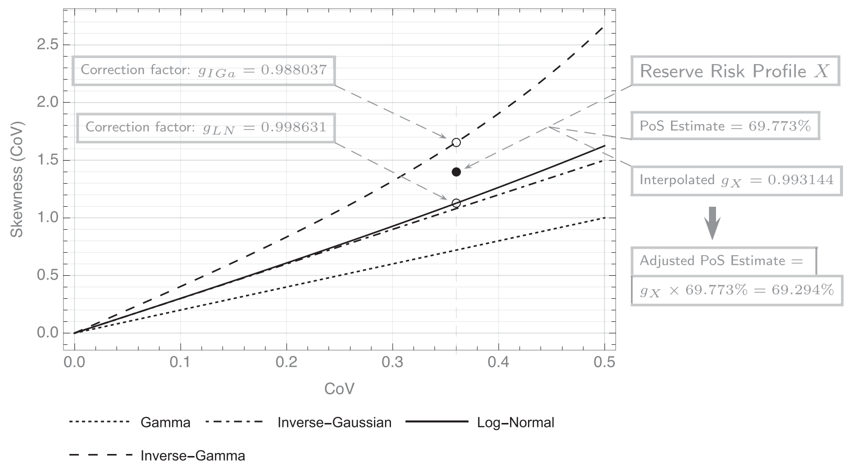

FIGURE 7: Numerical example: PoS estimate of standalone risk margin.

4. We compute the B-E estimate of PoS level of risk margin η_X of reserve risk profile F_X with volatility CoV_X and relative skewness SC_X. This has already been outputted in the table above in step 2, and equals $\widehat{\text{PoS}}_X = 69.773\%$. This estimate is then adjusted by the correction factor g_X obtained in the preceding step, and is equal to

$$\widetilde{\text{PoS}}_X = g_X \times \widehat{\text{PoS}}_X = 69.294\%.$$

The above steps are visualised in Figure 7.

6. CONCLUSIONS

The upcoming IFRS 17 brings one additional specific requirement to disclose confidence level of Solvency II reserve risk margins. This is no doubt an important requirement, and to be compliant with it in the future, insurers would need to start making the necessary preparations by estimating the effort needed to implement and accommodate this new upcoming regulatory requirement. However, at the moment, this is somewhat a remote issue for the majority of insurers as they are currently busy getting used to the requirements of the newly introduced Solvency II regime, and also because the IFRS 17 will commence only in early 2021.

In this paper, we take the first step in the actuarial research space and look out for practical ways of implementing this new requirement. In particular, we propose a distribution-free approach to estimating IFRS confidence level of Solvency II reserve risk margins in a "standard formula" style. Here, the risk margin confidence level measured by PoS is estimated by using only the key characteristics of the reserve risk profile: *(1) the level of variability measured*

https://doi.org/10.1017/asb.2017.12 Published online by Cambridge University Press

by coefficient of variation; (2) skewness; and, if necessary, *(3) kurtosis*. The PoS approximation formulae are derived for both the standalone reserving class risk margin and the diversified risk margin at the portfolio level. The quality of obtained PoS approximations was analysed, and it was shown that in most practical situations the approximations utilising CoV and skewness only, like B-E and C-F Quadratic approximations, are of fairly good quality, and that, only in very rare extreme situations when the reserve risk profile is overly skewed and leptokurtotic, the kurtosis becomes also a significant driver of the quality of approximation.

The CoV, skewness and kurtosis are invariant with respect to reserve risk profile location, i.e. *the reserve best estimate*, and hence are universal in categorising reserve risk profiles. By relating skewness and kurtosis to CoV level, we could trace the "statistical DNA" of reserve risk profiles to be able to locate them in the system of the four known parametric distributions that in principle cover a wide range of reserve risks. The four parametric distributions are used to derive correction factors to be applied to their corresponding distribution-free approximation of PoS to arrive at the theoretical value of PoS. Knowing the correction factors of the known parametric distributions that are in close proximity to the particular reserve risk profile, and also the distribution-free approximation of PoS of the reserve risk profile, allows us to arrive at the ultimate PoS approximation of fairly high quality.

Acknowledgement

The authors[20] would like to thank their colleagues from the International Actuarial Association (IAA) and the International Accounting Standards Board (IASB) for posing this interesting question about practical ways of estimating the confidence level of reserve risk margins. Also, Yuriy Krvavych thanks Anam Khan (Boston Consulting Group, London, UK) and Stephen Ryan (PwC, London, UK) for their critical review of early versions of this paper and invaluable comments, and also PwC for expressing interest and supporting this research work.

Notes

1. The *Best Estimate* is defined as a probability-weighted average (mean) of the present value of future liability cash flows. This estimate is unbiased, i.e. calculated with no prudence or optimism.
2. IFRS 17 is an upcoming International Financial Reporting Standard that is anticipated to be released in 2017. It will replace current IFRS 4 standard on accounting for insurance contracts and has an expected effective date of January 1, 2021.
3. Australian Prudential Regulation Authority.
4. More specifically, APRA Prudential Standards GPS 310 stipulate that the risk margin of a particular liability must be the greater of (a) half of the estimated standard deviation of the liability; and (b) the margin that provides 75% of PoS to meet the liability. As was shown in Taylor (2006), assuming log-normality of the reserve risk, the minimum APRA risk margin would be equivalent to 75th PoS level for most practically feasible values of reserve volatility, and turn to "half of the standard deviation" only in rare extreme situations.

5. In general, the statistical central estimate could be mean, mode or median. However, under APRA requirements, the central estimate is unbiased mean of insurance liabilities and is equivalent to Solvency II notion of best estimate.

6. The idea of applying a Gaussian dependence structure in reserve risk aggregation was earlier employed in Dal Moro (2013) and Dal Moro (2014) when deriving the moments of aggregate reserve risk across a multivariate log-normal reserve risk profile. This paper applies a Gaussian dependence structure to any multivariate distribution and derives the four moments of the aggregate reserve risk profile by using C-F and Fleishman approximations.

7. Fleishman approximation is a polynomial of a standard normal variable allowing to approximate non-normal distributions by utilising their moments of up to the fourth order.

8. For example, see Krvavych (2013).

9. Please refer to Kleiber and Kotz (2003), Nadarajah and Kotz (2006), Nadarajah (2011), Marshall and Olkin (2007) and Wolfram Documentation Center.

10. Here, kurtosis is regarded as excess-kurtosis and thus is defined via the fourth- and second-order cumulants of the reserve distribution.

11. It should be noted that the standard (Tweedie) parameterisation $IG(\mu, \lambda)$ is not of $\mathcal{SSP}$ type. However, the distribution can be reparameterised to become of $\mathcal{SSP}$ type by setting $\mu = \frac{\nu}{\theta}$ and $\lambda = \frac{\nu^2}{\theta}$ (e.g., see Marshall and Olkin, 2007). In this case, ν is the unique shape parameter.

12. Skewness and Kurtosis are, respectively, $\gamma(X) = \frac{\kappa_3(X)}{\kappa_2^{3/2}(X)}$ and $\iota(X) = \frac{\kappa_4(X)}{\kappa_2^2(X)}$ and are invariant with respect to centralisation and standardisation of X. Here, $\kappa_n(X)$ is the nth cumulant of X.

13. The detailed derivation of the C-F expansion can be found in Fisher and Cornish (1960) and Lee and Lee (1992). This paper assumes that the $\text{VaR}_\alpha\left(\widetilde{X}\right)$ can be well approximated by the moments of X of up to fourth order.

14. This requires existence of finite moments of reserve risk profile. It is assumed that in practice, reserving losses, including large liability losses, would realistically be bounded from above, therefore ensuring existence of finite moments.

15. $\mathcal{PD}$ was defined on page 743.

16. $\mathcal{A}$ was defined on page 750.

17. The detailed outputs of the analysis of quality of PoS approximations are provided in Appendix C.

18. As per our definition ι is defined via the fourth- and second-order cumulants and thus represents excess-kurtosis (used in the C-F expansion).

19. As per our definition ι is defined via the fourth- and second-order cumulants and thus represents excess-kurtosis (used in the C-F expansion). The fourth centralised moment of $P_2(Z_i)$ is simply the absolute kurtosis, hence ι is translated by 3.

20. **Disclaimer:** The views and opinions expressed in this article are those of the authors and do not reflect the official policy or position of SCOR and PwC.

REFERENCES

ABRAMOWITZ, M. and STEGUN, I.A. (1972) *Handbook of Mathematical Functions with Formulas, Graphs, and Mathematical Tables*, 9th edition. New York: Dover.

APRA PRUDENTIAL STANDARDS GPS 310. (2010) Audit and Actuarial Reporting and Valuation. *APRA*. Available at: http://www.apra.gov.au/gi/documents/gps-310-final-june-2010.pdf.

BABBEL, D.F., GOLD, J. and MERRILL, C.B. (2002) Fair value of liabilities: The financial economics perspective. *North American Actuarial Journal*, **6** (1), 12–27.

BATEUP, R. and REED, I. (2001) Research and data analysis relevant to the development of Standard Guidelines on liability valuation for general insurance. *XIII General Insurance Seminar*.

BOHMAN, H. and ESSCHER, F. (1963) Studies in risk theory with numerical illustrations concerning distribution functions and stop loss premiums. Part I. *Scandinavian Actuarial Journal*, **1963** (3–4), 173–225.

BOHMAN, H. and ESSCHER, F. (1964) Studies in risk theory with numerical illustrations concerning distribution functions and stop loss premiums. Part II. *Scandinavian Actuarial Journal*, **1964** (1–2), 1–40.

BÜHLMANN, H. (2004) Multidimensional valuation. *Finance*, **25**, 15–29.

CEIOPS. (2010) QIS5 Technical Specifications. Available at: https://eiopa.europa.eu/Publications/QIS/QIS5-technical_specifications_20100706.pdf.

CHRISTOFFERSEN, P. (2011) *Elements of Financial Risk Management*, 2nd edition. Waltham, MA: Academic Press.

DAL MORO, E. (2013) *A closed-form formula for the skewness estimation of non-life reserve risk distribution*. Working Paper. Available at: http://papers.ssrn.com/sol3/papers.cfm?abstract_id=2344297.

DAL MORO, E. (2014) *An approximation of the non-life reserve risk distributions using Cornish-Fisher expansion*. Working Paper. Available at: https://papers.ssrn.com/sol3/papers.cfm?abstract_id=2965384.

DAYKIN, C.D., PENTIKÄINEN, T. and PESONEN, M. (1994) *Practical Risk Theory for Actuaries*. UK: Chapman & Hall.

EMBRECHTS, P. and JACOBSONS, E. (2016) Dependence uncertainty for aggregate risk: Examples and simple bounds. In *The Fascination of Probability, Statistics and their Applications. In Honour of Ole E. Barndorff-Nielsen* (eds. M. Podolskij, S. T.A.V., R. Stelzer), pp. 395–417. Berlin: Springer.

EMBRECHTS, P., KLÜPPELBERG, C. and MIKOSCH, T. (2011) *Modelling Extremal Events: for Insurance and Finance*. UK: Springer.

EMBRECHTS, P., FREY, R. and MCNEIL, A. (2015) *Quantitative Risk Management: Concepts, Techniques and Tools*, 2nd edition. Princeton, NJ: Princeton University Press.

FINMA. (2006) Technical Document on the Swiss Solvency Test. Available at: https://www.finma.ch/FinmaArchiv/bpv/download/e/SST_techDok_061002_E_wo_Li_20070118.pdf.

FISHER, R.A. and CORNISH, E.A. (1960) The percentile points of distributions having known cumulants. *Technometrics*, **5**, 63–69.

FLEISHMAN, A.I. (1978) A method for simulating non-normal distributions. *Psychometrika*, **43**, 521–532.

GIJBELS, I. and HERRMANN, K. (2014) On the distribution of sums of random variables with copula-induced dependence. *Insurance: Mathematics and Economics*, **59**(C), 27–44.

GUY CARPENTER (2014) Insurance risk benchmark review. *Annual Statistical Review*. Available at: http://www.guycarp.com/content/dam/guycarp/en/documents/dynamic-content/Insurance_Risk_Benchmarks_Research_Annual_Statistical_Review.pdf.

HALDANE, J.B.S. (1938) The approximate normalization of a class of frequency distributions. *Biometrika*, **29**, 392–404.

IAA. (2009) Measurement of liabilities for insurance contracts: Current estimates and risk margins. *The International Actuarial Association*. Available at: http://www.actuaries.org/LIBRARY/Papers/IAA_Measurement_of_Liabilities_2009-public.pdf.

IASB. (2007) Preliminary views on insurance contracts. *IASB*. Available at: http://www.iasb.org.

ISSERLIS, L. (1918) On a formula for the product-moment coefficient of any order of a normal frequency distribution in any number of variables. *Biometrika*, **12**, 134–139.

KLEIBER, C. and KOTZ, S. (2003) *Statistical Size Distributions in Economics and Actuarial Sciences*, Wiley Series in Probability and Statistics, volume 381, 1st edition. New York, USA: Wiley-Interscience.

KOTZ, S., JOHNSON, N. and BALAKRISHNAN, N. (1994) *Continuous Univariate Distributions*, volume 1, 2nd edition. New York, USA: Wiley.

KRVAVYCH, Y. (2013) Making use of internal capital models. *ASTIN Colloquium, May 21–24, 2013, The Hague*. Available at: http://www.actuaries.org/ASTIN/Colloquia/Hague/Papers/Krvavych.pdf.

LEE, Y.-S. and LEE, M.C. (1992) On the derivation and computation of the Cornish-Fisher expansion. *Australian Journal of Statistics*, **34**, 443–450.

MARSHALL, A. and OLKIN, I. (2007) *Life Distributions: Structure of Nonparametric, Semiparametric, and Parametric Families*. Springer Series in Statistics. New York, USA: Springer.

MØLLER, T. (2004) Stochastic orders in dynamic reinsurance markets. *Finance and Stochastics*, **8**(4), 479–499.

Møller, T. and Steffensen, M. (2007) *Market-Valuation Methods in Life and Pension Insurance*. Cambridge: Cambridge University Press.
NADARAJAH, S. (2011) The exponentiated exponential distribution: a survey. *AStA Advances in Statistical Analysis*, **95**, 219–251.
NADARAJAH, S. and KOTZ, S. (2006) The exponentiated type distributions. *Acta Applicandae Mathematicae*, **92**, 97–111.
PENTIKÄINEN, T. (1987) Approximative evaluation of the distribution function of aggregate claims. *ASTIN Bulletin*, **17**, 15–39.
SALZMANN, R., WÜTHRICH, M. and MERZ, M. (2012) Higher moments of the claims development result in general insurance. *ASTIN Bulletin*, **42**, 355–384.
SANDSTRÖM, A. (2011) *Handbook of Solvency for Actuaries and Risk Managers*. UK: Chapman & Hall.
SCOR. (2008) *From Principle-Based Risk Management to Solvency Requirements: Analytical Framework for the Swiss Solvency Test*. Switzerland: SCOR.
SEAL, H. (1977) Approximations to risk theory's $f(x, t)$ by means of the gamma distribution. *ASTIN Bulletin*, **9**, 213–218.
SHMAKOV, S. (2011) A universal method of solving quartic equations. *International Journal of Pure and Applied Mathematics*, **71**(2), 251–259.
SST. (2004) White paper of the Swiss Solvency Test. *Swiss Federal Office for Private Insurance*. Available at: https://www.finma.ch/FinmaArchiv/bpv/download/e/WhitePaperSST_en.pdf.
STROMMEN, S.J. (2006) Setting the levels of margins in a principle-based valuation using a cost-of-capital approach with exponential utility. *The Financial Reporter*, **2006** (65).
TAYLOR, G. (2006) APRA general insurance risk margins. *Australian Actuarial Journal*, **12** (3), 367–397.
WILSON, E.B. and HILFERTY, M. (1931) The distribution of chi-square. *Proceedings of the National Academy of Science*, **17**, 684–688.
WOLFRAM DOCUMENTATION CENTER. Parametric statistical distributions. Available at: http://reference.wolfram.com/language/guide/ParametricStatisticalDistributions.html.
WÜTHRICH, M., BÜHLMANN, H. and FURRER, H. (2007) *Market-Consistent Actuarial Valuation*. Heidelberg: Springer.

ERIC DAL MORO (Corresponding author)
Actuarial Reserving
SCOR 26 General Guisan-Quai
CH-8022 Zurich, Switzerland
E-Mail: EDalMoro@scor.com

YURIY KRVAVYCH
Actuarial and Insurance Management Solutions
PwC UK, 7 More London Riverside,
London SE1 2RT, UK
E-Mail: yuriy.krvavych@uk.pwc.com

APPENDIX A: TABULATED FLEISHMAN COEFFICIENTS

The Fleishman coefficients of the polynomial $P_3(Z) = aZ + b\left(Z^2 - 1\right) + cZ^3$ of a standard normal random variable Z are calibrated in such a way that

https://doi.org/10.1017/asb.2017.12 Published online by Cambridge University Press

TABLE A1

FLEISHMAN COEFFICIENTS FOR THE FOUR PARAMETRIC DISTRIBUTIONS FROM $\mathcal{PD}$.

	Gamma			Inverse-Gaussian		
CoV	a	b	c	a	b	c
5%	0.7821269	0.0114362	0.0679523	0.7816586	0.0171455	0.0680652
10%	0.7814394	0.0228591	0.0680955	0.7795694	0.0342187	0.0685466
15%	0.7802942	0.0342555	0.0683341	0.7760992	0.0511486	0.0693467
20%	0.7786927	0.0456123	0.0686680	0.7712656	0.0678665	0.0704621
25%	0.7766366	0.0569165	0.0690971	0.7650925	0.0843071	0.0718882
30%	0.7741280	0.0681552	0.0696211	0.7576098	0.1004096	0.0736193
35%	0.7711696	0.0793157	0.0702400	0.7488526	0.1161185	0.0756483
40%	0.7677644	0.0903856	0.0709533	0.7388605	0.1313843	0.0779670
45%	0.7639159	0.1013527	0.0717609	0.7276770	0.1461641	0.0805664
50%	0.7596281	0.1122051	0.0726623	0.7153487	0.1604223	0.0834364

	Log-Normal			Inverse-Gamma		
CoV	a	b	c	a	b	c
5%	0.7815348	0.0171566	0.0681015	0.7806977	0.0228912	0.0683124
10%	0.7790443	0.0343063	0.0686994	0.7755591	0.0458618	0.0695806
15%	0.7748059	0.0514359	0.0697200	0.7664274	0.0689512	0.0718487
20%	0.7686882	0.0685194	0.0711998	0.7523662	0.0921107	0.0753724
25%	0.7605075	0.0855125	0.0731893	0.7318810	0.1151398	0.0805574
30%	0.7500289	0.1023471	0.0757533	0.7027094	0.1376087	0.0880106
35%	0.7369696	0.1189283	0.0789696	0.6615037	0.1587849	0.0986036
40%	0.7210045	0.1351332	0.0829261	0.6033250	0.1776160	0.1135503
45%	0.7017757	0.1508147	0.0877178	0.5206582	0.1928308	0.1345288
50%	0.6789048	0.1658095	0.0934413	0.4009040	0.2031524	0.1640103

$$
\begin{aligned}
&\mathbb{E}\left[P_3^2(Z)\right] = a^2 + 6ac + 15c^2 = 1; \\
&\mathbb{E}\left[P_3^3(Z)\right] = 2b\left(a^2 + 24ac + 105c^2 + 2\right) = \gamma; \\
&\mathbb{E}\left[P_3^4(Z)\right] = 24\left[ac + b^2\left(1 + a^2 + 28ac\right)\right. \\
&\qquad\qquad \left. + c^2\left(12 + 48ac + 141b^2 + 225c^2\right)\right] = \iota + 3.
\end{aligned}
\tag{A1}
$$

For a given risk profile with level of variability CoV, we find the corresponding values of $\gamma(\text{CoV})$ and $\iota(\text{CoV})$ and solve the system of equations (A1).

The Table A1 provides calibrated Fleishman coefficients for each of the four parametric distribution from $\mathcal{PD}$ at different levels of CoV.

If necessary, the Fleishman coefficients can be pre-computed at much higher resolution of CoV and $\mathcal{PD}$.

APPENDIX B: DERIVATION OF SKEWNESS AND KURTOSIS AT THE PORTFOLIO LEVEL

The derivation of approximations of skewness and kurtosis of the aggregate reserve risk is based on the assumption that standalone reserve risk profiles are approximated with the Fleishman polynomial of a standard normal random variable and follow a Gaussian dependence structure. This implies a multivariate normal distribution and calculating moments of multivariate polynomial function of a multivariate normal distribution. In particular, the components of skewness and kurtosis approximation formulae for the reserve risk portfolio are of the following types:

$$\mathbb{E}\left[P_3(Z_i)^{n_i} P_3(Z_j)^{n_j} P_3(Z_k)^{n_k} P_3(Z_l)^{n_l}\right]$$

with $n_i, n_j, n_k, n_l \geqslant 0$ and $n_i + n_j + n_k + n_l \leqslant 4$. This reduces to calculating high-order moments of the multivariate standard normal distribution:

$$\mathbb{E}\left[Z_i^{n_i} Z_j^{n_j} Z_k^{n_k} Z_l^{n_l}\right]$$

with $n_i, n_j, n_k, n_l \geqslant 0$ and $n_i + n_j + n_k + n_l \leqslant 12$. The multivariate standard normal moments for which $n_i + n_j + n_k + n_l$ is odd are equal to zero. When $n_i + n_j + n_k + n_l$ is even the high-order moment of a multivariate standard normal is then calculated using Isserlis's Formula. The Isserlis' Formula is defined and used to compute high-order moments of multivariate standard normal random variables in Isserlis (1918).

APPENDIX C: ANALYSIS OF QUALITY OF APPROXIMATIONS — DETAILED OUTPUTS

This appendix provides a small sample of detailed outputs from the analysis of quality of PoS approximations. In particular, the detailed outputs for Inverse-Gamma under the assumption of $\eta = 25\%$ are tabulated and visualised below in Table C1 and Figure C1. These outputs cover cases 16 and 17 analysed in Section 3.4 and discussed on page 767.

The full set of detailed outputs from the analysis of quality of PoS approximations can be downloaded from https://drive.google.com/open?id=0B6piPKdUSkYISWRWMEkzZ3VlWmc (please refer to Appendix C therein).

https://doi.org/10.1017/asb.2017.12 Published online by Cambridge University Press

TABLE C1

POS OF INVERSE-GAMMA DISTRIBUTION WITH $\eta = 25\%$: ACTUAL VS. APPROXIMATED.

CoV =	Parametric Distrib	B-E Approx	C-F Quadr Approx	C-F Cubic Approx	C-F Quartic Approx	B-E Approx Δ %	Quadr Approx Δ %	Cubic Approx Δ %	Quartic Approx Δ %
5%	0.99999	0.99999	0.99999	0.99999	0.99999	−0.00011	−0.00013	−4.49E−06	−0.00019
10%	0.98718	0.98734	0.98719	0.98702	0.98701	−0.01624	−0.00105	0.01561	0.01743
15%	0.93988	0.93873	0.93694	0.93923	0.93482	0.12176	0.31309	0.06859	0.54147
20%	0.89132	0.88801	0.88330	0.89129	0.87966	0.37334	0.90813	0.00335	1.32569
25%	0.85446	0.84968	0.84134	0.85757	0.83886	0.56338	1.55924	−0.36220	1.86051
30%	0.82852	0.82373	0.81114	0.83863	0.81279	0.58121	2.14276	−1.20554	1.93471
35%	0.81068	0.80780	0.79017	0.83336	0.79790	0.35640	2.59508	−2.72188	1.60092
40%	0.79855	0.79984	0.77619	0.84143	0.79004	−0.16040	2.88109	−5.09551	1.07793
45%	0.79044	0.79845	0.76755	0.86226	0.78565	−1.00354	2.98097	−8.32981	0.60879
50%	0.78513	0.80273	0.76312	0.89143	0.78236	−2.19240	2.88467	−11.92440	0.35398

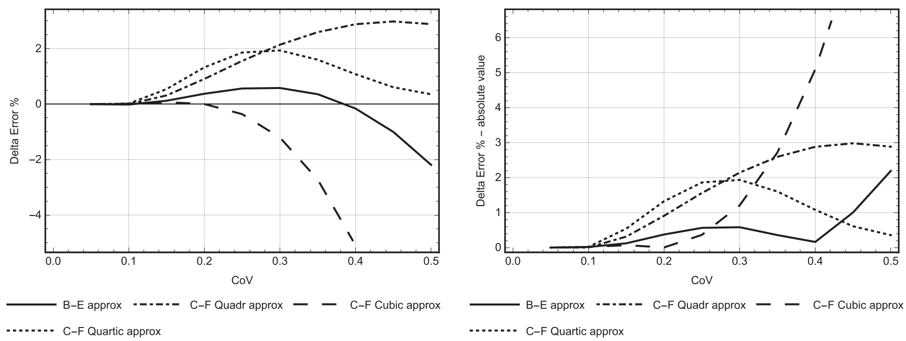

(a) Δ %

(b) $|\Delta|$ %

FIGURE C1: PoS of Inverse-Gamma distribution with $\eta = 25\%$: delta error. (a) Δ %. (b) $|\Delta|$ %.

https://doi.org/10.1017/asb.2017.12 Published online by Cambridge University Press